

Multiple competition-based FDR control for peptide detection

Kristen Emery¹, Syamand Hasam¹, William Stafford Noble², Uri Keich¹

¹School of Mathematics and Statistics F07

University of Sydney

²Departments of Genome Sciences and of Computer Science and Engineering

University of Washington

November 14, 2019

Abstract

Competition-based FDR control has been commonly used for over a decade in the computational mass spectrometry community (Elias and Gygi, 2007). Recently, the approach has gained significant popularity in other fields after Barber and Candès (2015) laid its theoretical foundation in a more general setting that included the feature selection problem. In both cases, the competition is based on a head-to-head comparison between an observed score and a corresponding decoy / knockoff. Keich and Noble (2017b) recently demonstrated some advantages of using multiple rather than a single decoy when addressing the problem of assigning peptide sequences to observed mass spectra. In this work, we consider a related problem — detecting peptides based on a collection of mass spectra — and we develop a new framework for competition-based FDR control using multiple null scores. Within this framework, we offer several methods, all of which are based on a novel procedure that rigorously controls the FDR in the finite sample setting. Using real data to study the peptide detection problem we show that, relative to existing single-decoy methods, our approach can increase the number of discovered peptides by up to 50% at small FDR thresholds.

KEYWORDS: multiple hypothesis testing, peptide detection, tandem mass spectrometry, false discovery rate

1 Introduction

Proteins are the primary functional molecules in living cells, and tandem mass spectrometry (MS/MS) currently provides the most efficient means of studying proteins in a high-throughput fashion. Knowledge of the protein complement in a cellular population provides insight into the functional state of the cells. Thus, MS/MS can be used to functionally characterize cell types, differentiation stages, disease states, or species-specific differences. For this reason, MS/MS is the driving technology for much of the rapidly growing field of proteomics.

Paradoxically, MS/MS does not measure proteins directly. Because proteins themselves are difficult to separate and manipulate biochemically, an MS/MS experiment involves first digesting proteins into smaller pieces, called “peptides.” The peptides are then measured directly. A typical MS/MS experiment generates ~ 10 observations (“spectra”) per second, so a single 30-minute

MS/MS experiment will generate approximately 18,000 spectra. Canonically, each observed spectrum is generated by a single peptide. Thus, the first goal of the downstream analysis is to infer which peptide was responsible for generating each observed spectrum. The resulting set of detected peptides can then be used, in a second analysis stage, to infer what proteins are present in the sample.

In this work, we are interested in the first problem — peptide detection. Specifically, we focus on the task of assigning confidence estimates to peptides that have been identified by MS/MS. As is common in many molecular biology contexts, these confidence estimates are typically reported in terms of the false discovery rate (FDR), i.e., the expected value of the proportion of false discoveries among a set of detected peptides. For reasons that will be explained below, rather than relying on standard methods for control of the FDR such as the Benjamini and Hochberg (1995) (BH) procedure the proteomics field employs a strategy known as “target-decoy competition” (TDC) to control the FDR in the reported list of detected peptides (Elias and Gygi, 2007). TDC works by comparing the list of peptides detected with a list of artificial peptides, called “decoys,” detected using the same spectra set. The decoys are created by reversing or randomly shuffling the letters of the real (“target”) peptides. The TDC protocol, which is described in detail in Section 2.2, estimates the FDR by counting the number of detected decoy peptides and using this count as an estimate for the number of incorrectly detected target peptides.

One clear deficiency of TDC is its reliance on a single set of decoy peptides to estimate the FDR. Thus, with ever increasing computational resources one can ask whether we can gain something by exploiting multiple randomly drawn decoys for each target peptide. Keich and Noble (2017b) and Keich, Tamura, and Noble (2018) recently described such a procedure, called “average target-decoy competition” (aTDC), that, in the context of the related spectrum identification problem (described in Section 2.1), reduces the variability associated with TDC and can provide a modest boost in power.

In this paper we propose a new approach to using multiple decoy scores. The proposed procedure relies on a direct competition between the target and its corresponding decoy scores, rather than on averaging single competitions. We formulate our approach in the following more general setting. Suppose that we can compute a test statistic Z_i for each null hypothesis H_i , so that the larger Z_i is, the less likely is the null. However, departing from the standard multiple hypotheses setup, we further assume that we cannot compute p-values for the observed scores. Instead, we can only generate a *small* sample of independent decoys or competing null scores for each hypothesis H_i : \tilde{Z}_i^j $j = 1, \dots, d$ (Definition 2). Note that the case $d = 1$ corresponds to the TDC setup described above. We will show using both simulated and real data that the novel method we propose yields more power (more discoveries) than our aforementioned averaging procedure.

In addition to the peptide detection problem, our proposed procedure is applicable in several other bioinformatics applications. For example, the procedure could be used when analyzing a large number of motifs reported by a motif finder, e.g., Harbison et al. (2004), where creating competing null scores can require the time consuming task of running the finder on randomized versions of the input sets, e.g., Ng and Keich (2008). In addition, our procedure is applicable to controlling the FDR in selecting differentially expressed genes in microarray experiments where a small number of permutations is used to generate competing null scores (Tusher, Tibshirani, and Chu, 2001).

Our proposed method can also be viewed as a generalization of the “knockoff” procedure of Barber and Candès (2015). The knockoff procedure is a competition-based FDR control method that was initially developed for feature selection in a classical linear regression model. The procedure has gained a lot of interest in the statistical and machine learning communities, where it has

been applied to various applications in biomedical research (Xiao et al., 2017; Gao et al., 2018; Read et al., 2019) and has been extended to work in conjunction with deep neural networks (Lu et al., 2018) and with time series data (Fan et al., 2018). Despite the different terminology, both knockoffs and decoys serve the same purpose in competition-based FDR control; hence, for the ideas presented in this paper the two are interchangeable.

A significant part of Barber and Candés’ work is the sophisticated construction of their knockoff scores; controlling the FDR then follows exactly the same competition that TDC uses. Indeed, their Selective SeqStep+ (SSS+) procedure rigorously formalizes in a much more general setting the same procedure described above in the context of TDC.

Note that Barber and Candés suggested that using multiple knockoffs could improve the power of their procedure so the methods we propose here could provide a stepping stone toward that. However, we would still need to figure out how to generalize their construction from one to multiple knockoffs.

2 Background

By way of background, we begin with a brief description of the mass spectrometry protocol and outline how the resulting spectra are assigned to peptides. We then discuss existing methods for statistical confidence estimation, and we introduce the peptide detection problem which is the focus of our work.

2.1 Shotgun proteomics and spectrum identification

In a “shotgun proteomics” MS/MS experiment, proteins in a complex biological sample are extracted and digested into peptides, each with an associated charge. These charged peptides, called “precursors,” are measured by the mass spectrometer, and a subset of the precursors are then selected for further fragmentation into charged ions, which are detected and recorded by a second round of mass spectrometry (P. Hernandez and Appel, 2006; Noble and MacCoss, 2012). The recorded tandem fragmentation spectra, or spectra for short, are then subjected to computational analysis.

This analysis typically begins with the spectrum identification problem, which involves inferring which peptide was responsible for generating each observed fragmentation spectrum. The most common solution to this problem is peptide database search. Pioneered by SEQUEST (Eng et al., 1994), the search engine extracts from the peptide database all “candidate peptides,” defined by having their mass lie within a pre-specified tolerance of the measured precursor mass. The quality of the match between each one of these candidate peptides and the observed fragmentation spectrum is then evaluated using a score function. Finally, the optimal peptide-spectrum match (PSM) for the given spectrum is reported, along with its score (Nesvizhskii, 2010).

In practice, many expected fragment ions will fail to be observed for any given spectrum, and the spectrum is also likely to contain a variety of additional, unexplained peaks (Noble and MacCoss, 2012). Hence, sometimes the reported PSM is correct — the peptide assigned to the spectrum was present in the mass spectrometer when the spectrum was generated — and sometimes the PSM is incorrect. Ideally, we would report only the correct PSMs, but obviously we are not privy to this information: all we have is the score of the PSM, indicating its quality. Therefore, we report a

thresholded list of top-scoring PSMs, together with the critical estimate of the fraction of incorrect PSMs in our reported list.

2.2 False discovery rate control in spectrum identification

The general problem of controlling the proportion of false discoveries has been studied extensively in the context of multiple hypotheses testing (MHT). Briefly reviewed in Section 3.1 below, this setup does not apply directly to the spectrum identification problem. A major reason for that is the presence in any shotgun proteomics dataset of both “native spectra” (those for which their generating peptide is in the target database) and “foreign spectra” (those for which it is not). These create different types of false positives, implying that we typically cannot apply FDR controlling procedures that were designed for the general MHT context to the spectrum identification problem (Keich and Noble, 2017a).

Instead, the mass spectrometry community uses TDC to control the FDR in the reported list of PSMs (Elias and Gygi, 2007; Cerqueira et al., 2010; Jeong et al., 2012; Elias and Gygi, 2010). TDC works by comparing searches against a target peptide database with searches against a decoy database of peptides obtained from the original database by randomly shuffling (or reversing) each peptide in the target database.

More precisely, let Z_i be the score of the optimal match (PSM) to the i th spectrum in the target database, and let \tilde{Z}_i be the corresponding optimal match in the decoy database. Each decoy score \tilde{Z}_i directly competes with its corresponding target score Z_i for determining the reported list of discoveries. Specifically, for each score threshold T we only report target PSMs that won their competition: $Z_i > \max\{T, \tilde{Z}_i\}$. Subsequently, the number of decoy wins ($\tilde{Z}_i > \max\{T, Z_i\}$) is used to estimate the number of false discoveries in the list of target wins. Thus, the ratio between that estimate and the number of target wins yields an estimate of the FDR among the target wins. To control the FDR at level α we choose the smallest threshold $T = T(\alpha)$ for which the estimated FDR is still $\leq \alpha$.

It was recently shown that, assuming that incorrect PSMs are independently equally likely to come from a target or a decoy match and provided we add 1 to the number of decoy wins before dividing by the number of target wins, this procedure rigorously controls the FDR (He et al., 2015; Levitsky et al., 2017).

2.3 The peptide detection problem

The spectrum identification is largely used as the first step in addressing the peptide identification problem that motivates the research presented here. Indeed, to identify the peptides we begin, just like we do in spectrum identification, by assigning each spectrum to the unique target/decoy peptide which offers the best match to this spectrum in the corresponding database. We then assign to each target peptide a score Z_j which is the maximum of all PSM scores of spectra that were assigned to this peptide in the first phase. Similarly, we assign to the corresponding decoy peptide a score \tilde{Z}_j , which again is the maximum of all PSM scores involving spectra that were assigned to that decoy peptide. The rest continues using the same TDC protocol we outlined above for the spectrum identification problem (Granhölm et al., 2013; Savitski et al., 2015).

3 Controlling the FDR using multiple decoys

3.1 Why do we need a new approach?

In the multiple hypotheses testing (MHT) set up we simultaneously test m (null) hypotheses H_1, \dots, H_m , looking to reject as many as possible subject to some statistical control of our error rate. Pioneered by Benjamini and Hochberg, the common approach to controlling the error rate in the MHT context is through bounding the expected proportion of false discoveries at any desired level $\alpha \in (0, 1)$.

More precisely, assume we have a selection procedure that produces a list of R discoveries of which, unknown to us, V are false, and let $Q = V / \max\{R, 1\}$ be the unobserved false discovery proportion (FDP). Benjamini and Hochberg (1995) showed that applying their selection procedure (BH) at level α controls $E(Q)$, the false discovery rate (FDR): $E(Q) \leq \alpha$.

Other, more powerful selection procedures that rely on estimating π_0 , the fraction of true null hypotheses, are available. Generally referred to as “adaptive BH” procedures, with one particularly popular variant by Storey, these procedures are also predicated on our ability to assign a p-value to each of our tested hypotheses (e.g., Benjamini and Hochberg, 2000; Benjamini, Krieger, and Yekutieli, 2006; Storey, 2002; Storey, Taylor, and Siegmund, 2004). Hence, in particular they cannot be directly applied in our competition-based setup.

A key feature of our problem is that due to computational costs the number of decoys, d , is small. Indeed, if we are able to generate a large number of independent decoys for each hypothesis, then we can simply apply the above standard FDR controlling procedures to the empirical p-values. These p-values are estimated from the empirical null distributions, which are constructed for each hypothesis H_i using its corresponding decoys. Specifically, these empirical p-values take values of the form $(d_1 - r_i + 1)/d_1$, where $d_1 = d + 1$, and $r_i \in \{1, \dots, d_1\}$ is the rank of the originally observed score (“original score” for short) Z_i in the combined list of d_1 scores: $(\tilde{Z}_i^0 = Z_i, \tilde{Z}_i^1, \dots, \tilde{Z}_i^d)$ ($r_i = 1$ is the lowest rank). Using these p-values the BH procedure rigorously controls the FDR, and Storey’s method will asymptotically control the FDR as the number of hypotheses $m \rightarrow \infty$.

Unfortunately, because d is small, applying those standard FDR control procedures to the rather coarse empirical p-values may yield very low power. For example, if $d = 1$, each empirical p-value is either 1/2 or 1, and therefore for many practical examples both methods will not be able to make any discoveries at usable FDR thresholds.

Alternatively, one might consider pooling all the decoys regardless of which hypothesis generated them. The pooled empirical p-values attain values of the form $i / (m \cdot d + 1)$ for $i = 1, \dots, md + 1$; hence, particularly when m is large, the p-values generally no longer suffer from being too coarse. However, other significant problems arise when pooling the decoys. These issues — discussed in Supplementary Section 6.1 — imply that in general, applying BH or Storey’s procedure to p-values that are estimated by pooling the competing null scores can be problematic both in terms of power and control of the FDR.

3.2 A novel meta-procedure for FDR control using multiple decoys

The main technical contribution of this paper is the introduction of several procedures that effectively control the FDR in our multiple competition-based setup and that rely on the following meta-procedure.

Input: an original/target score Z_i and d competing null scores \tilde{Z}_i^j for each null hypothesis H_i .

Parameters: an FDR threshold $\alpha \in (0, 1)$, two tuning parameters $c = i_c/d_1$ ($d_1 = d + 1$), the ‘‘original/target win’’ threshold, and $\lambda = i_\lambda/d_1$, the ‘‘decoy win’’ threshold where $i_\lambda, i_c \in \{1, \dots, d\}$ and $c \leq \lambda$, as well as a (possibly randomized) mapping function $\varphi : \{1, \dots, d_1 - i_\lambda\} \mapsto \{d_1 - i_c + 1, \dots, d_1\}$.

Procedure:

1. Each hypothesis H_i is assigned an original/decoy win label:

$$L_i = \begin{cases} 1 & r_i \geq d_1 - i_c + 1 & \text{(original win)} \\ 0 & r_i \in (d_1 - i_\lambda, d_1 - i_c + 1) & \text{(ignored hypothesis)} \\ -1 & r_i \leq d_1 - i_\lambda & \text{(decoy win)} \end{cases}, \quad (1)$$

where $r_i \in \{1, \dots, d_1\}$ is the rank of the original score when added to the list of its d decoy scores.

2. Each hypothesis H_i is assigned a score $W_i = \tilde{Z}_i^{(s_i)}$, where $\tilde{Z}_i^{(j)}$ is the j th order statistic or the j th largest score among $(\tilde{Z}_i^0 = Z_i, \tilde{Z}_i^1, \dots, \tilde{Z}_i^d)$, and the ‘‘selected rank’’, s_i , is defined as

$$s_i = \begin{cases} r_i & L_i = 1 \text{ (so } W_i = Z_i \text{ in an original win)} \\ u_i & L_i = 0 \text{ (where } u_i \text{ is randomly chosen uniformly in } \{d_1 - i_c + 1, \dots, d_1\}) \\ \varphi(r_i) & L_i = -1 \text{ (so } W_i \text{ coincides with a decoy score in a decoy win)} \end{cases} \quad (2)$$

3. The hypotheses are reordered so that W_i are decreasing, and the list of discoveries is defined as the subset of original wins $D(\alpha, c, \lambda) := \{i : i \leq i_{\alpha c \lambda}, L_i = 1\}$, where

$$i_{\alpha c \lambda} := \max \left\{ i : \frac{1 + \#\{j \leq i : L_j = -1\}}{\#\{j \leq i : L_j = 1\} \vee 1} \cdot \frac{c}{1 - \lambda} \leq \alpha \right\}. \quad (3)$$

We assume above that all ties in determining the ranks r_i , as well as the order of W_i , are broken randomly, although other ways to handle ties are possible (e.g., Section 8.3 in our technical report (Emery et al., 2019)).

Note that the hypotheses for which $L_i = 0$ can effectively be ignored as they cannot be considered discoveries nor do they factor in the numerator of (3).

Our procedures vary in how they define the (generally randomized) mapping function φ (and hence s_i in (2)), as well as in how they set the tuning parameters c, λ . For example, in the case $d = 1$ setting $c = \lambda = 1/2$ and $\varphi(1) := 2$ our meta-procedure coincides with TDC. For $d > 1$ we have increasing flexibility with d , but one obvious generalization of TDC is to set $c = \lambda = 1/d_1$. In this case $L_i = 1$ if the original score is larger than all its competing decoys and otherwise $L_i = -1$. Thus, by definition, φ is constrained to the constant value d_1 so $s_i \equiv d_1$ and W_i is always set to $Z_i^{(d_1)} = \max \{\tilde{Z}_i^0, \dots, \tilde{Z}_i^d\}$. Hence we refer to this as the ‘‘max method.’’ As we will see, the max method controls the FDR, but this does not hold for any choice of c, λ and φ . The following section specifies a sufficient condition on c, λ and φ that guarantees FDR control.

3.3 Null labels conditional probabilities property

Definition 1. Let N be the indices of all true null hypotheses. We say the null labels conditional probabilities property (NLCP) is satisfied if conditional on all the scores $\mathcal{W} = (W_1, \dots, W_m)$ the random labels $\{L_i : i \in N\}$ are (i) independent and identically distributed (iid) with $P(L_i = 1 | \mathcal{W}) = c$ and $P(L_i = -1 | \mathcal{W}) = 1 - \lambda$, and (ii) independent of the false null labels $\{L_i : i \notin N\}$.

Note that in claiming that TDC controls the FDR we implicitly assume that a false match is equally likely to arise from a target win as it is from a decoy win independently of all other scores (He et al., 2015). This property coincides with the NLCP with $d = 1$ and $c = \lambda = 1/2$. Our next theorem shows that the NLCP generally guarantees the FDR control of our meta-procedure. Specifically, we argue that with NLCP established step 3 of our meta-procedure can be viewed as a special case of Barber and Candès (2015)'s SSS+ procedure and its extension by Lei and Fithian (2016)'s Adaptive SeqStep (AS). Both procedures are designed for sequential hypothesis testing where the order of the hypotheses is pre-determined – by the scores W_i in our case.

Theorem 1. *If the NLCP holds then our meta-procedure controls the FDR in a finite-sample setting, that is, $E(|D(\alpha, c, \lambda) \cap N|/|D(\alpha, c, \lambda)|) \leq \alpha$, where the expectation is taken with respect to all the decoy draws.*

Why does Theorem 1 make sense? If the NLCP holds then a true null H_i is an original win ($L_i = 1$) with probability c and is a decoy win with probability $1 - \lambda$. Hence, the factor $\frac{c}{1-\lambda}$ that appears in (3) adjusts the observed number of decoy wins, $\#\{j \leq i : L_j = -1\}$, to estimate the number of (unobserved) false original wins (those for which the corresponding H_i is a true null). Ignoring the +1 correction, the adjusted ratio of (3) therefore estimates the FDR in the list of the first i original wins. The procedure simply takes the largest such list for which the estimated FDR is $\leq \alpha$.

Proof. To see the connection with SSS+ and AS we assign each hypothesis H_i a p-value $p_i := P(L_i \geq l)$. Clearly, if the NLCP holds then

$$p_i = \begin{cases} c & l = 1 \\ \lambda & l = 0 \\ 1 & l = -1 \end{cases} . \quad (4)$$

Moreover, the NLCP further implies that for any $u \in (0, 1)$ and $i \in N$, $P(p_i \leq u | \mathcal{W}) \leq u$, and that the true null labels L_i , and hence the true null p-values, p_i , are independent conditionally on \mathcal{W} .

It follows that, even after sorting the hypotheses by the decreasing order of the scores W_i , the p-values of the true null hypotheses are still iid valid p-values that are independent from the false nulls. Hence our result follows from Theorem 3 (SSS+) of Barber and Candès (2015) for $c = \lambda$, and more generally for $c \leq \lambda$ from Theorem 1 (AS) of Lei and Fithian (2016) (with $s = c$). \square

Remark 1. With the risk of stating the obvious we note that one cannot simply apply SSS+ or AS by selecting $W_i = Z_i$ for all i with the corresponding empirical p-values $(d_1 - r_i + 1)/d_1$. Indeed, in this case the order of the hypotheses (by W_i) is not independent of the true null p-values.

3.4 When does the NLCP hold for our meta-procedure?

To further analyze the NLCP we make the following assumption on our decoys.

Definition 2 (formalizing the multiple-decoy problem). If the d_1 (original and decoy) scores corresponding to each true null hypothesis are iid independently of all other scores then we say we have “iid decoys”.

It is clear that if we have iid decoys then for each fixed $i \in N$ the rank r_i is uniformly distributed on $1, \dots, d_1$, and hence $P(L_i = 1) = c$ and $P(L_i = -1) = 1 - \lambda$. However, to determine whether or not r_i is still uniformly distributed when conditioning on \mathcal{W} we need to look at the mapping function φ as well.

More specifically, in the iid decoys case the conditional distribution of $\{L_i : i \in N\}$ given \mathcal{W} clearly factors into the product of the conditional distribution of each true null L_i given W_i : a true null's L_i is independent of all $\{L_j, W_j : j \neq i\}$. Thus, it suffices to show that L_i is independent of W_i for each $i \in N$. Moreover, because W_i is determined in terms of s_i and the set of scores $\{\tilde{Z}_i^0, \dots, \tilde{Z}_i^d\}$, and because a true null's label L_i and s_i are independent of the last set (a set is unordered), it suffices to show that L_i is independent of s_i . Of course, s_i is determined by φ as specified in (2).

For example, consider the max method where $s_i \equiv d_1$ (equivalently $\varphi \equiv d_1$): in this case, L_i is trivially independent of s_i and hence by the above discussion the method controls the FDR. In contrast, assuming d_1 is even and choosing $\varphi \equiv d_1$ with $c = \lambda = 1/2$ we see that the scores $\{W_i : i \in N, L_i = -1\}$ will generally be larger than the corresponding $\{W_i : i \in N, L_i = 1\}$. Indeed, when $L_i = -1$ we always choose the maximal score $W_i = Z_i^{(d_1)}$, whereas W_i is one of the top half scores when $L_i = 1$. Hence, $P(L_i = -1 \mid \text{higher } W_i) > 1/2$.

So how can we guarantee that the NLCP holds for pre-determined values of $c = i_c/d_1$ and $\lambda = i_\lambda/d_1$? The next theorem provides a sufficient condition on φ (equivalently on s_i) to ensure the property holds.

Theorem 2. *If the iid decoys assumption holds, and if for any $i \in N$ and $j \in \{d_1 - i_c + 1, \dots, d_1\}$*

$$P(s_i = j, r_i \leq d_1 - i_\lambda) = P(s_i = j, L_i = -1) = \frac{d_1 - i_\lambda}{d_1 \cdot i_c}, \quad (5)$$

then the NLCP holds and hence our meta-procedure with those values of c, λ and φ controls the FDR.

Proof. By (5), for any $i \in N$ and $j \in \{d_1 - i_c + 1, \dots, d_1\}$,

$$\begin{aligned} P(L_i = 1 \mid s_i = j) &= \frac{P(s_i = j, L_i = 1)}{\sum_{l \in \{-1, 0, 1\}} P(s_i = j, L_i = l)} \\ &= \frac{1/d_1}{(d_1 - i_\lambda)/(d_1 \cdot i_c) + (i_\lambda - i_c)/d_1 \cdot 1/i_c + 1/d_1} = \frac{i_c}{d_1} = c, \\ P(L_i = -1 \mid s_i = j) &= \frac{(d_1 - i_\lambda)/(d_1 \cdot i_c)}{(d_1 - i_\lambda)/(d_1 \cdot i_c) + (i_\lambda - i_c)/d_1 \cdot 1/i_c + 1/d_1} = \frac{d_1 - i_\lambda}{d_1} = 1 - \lambda. \end{aligned}$$

At the same time $P(L_i = 1 \mid s_i = j) = 1$ for $j \in \{1, \dots, i_c\}$ always holds; therefore, L_i is independent of s_i and by the above discussion the NLCP holds. Theorem 1 completes the proof. \square

For any fixed values of c, λ we can readily define a randomized $\varphi = \varphi_u$ so that the NLCP holds: randomly and uniformly map $\{1, \dots, d_1 - i_\lambda\}$ onto $\{d_1 - i_c + 1, \dots, d_1\}$. Indeed, in this case (5) holds:

$$P(s_i = j, s_i \neq r_i) = P(r_i \in \{1, \dots, d_1 - i_\lambda\}) \cdot P(s_i = j \mid r_i \in \{1, \dots, d_1 - i_\lambda\}) = \frac{d_1 - i_\lambda}{d_1} \cdot \frac{1}{i_c}. \quad (6)$$

3.5 Mirroring and Mirandom

Using the above randomized uniform map φ_u we have a way to define an FDR-controlling variant of our meta-procedure for any pre-determined c, λ . However, we can design more powerful procedures using alternative definitions of φ (for the same values of c, λ).

For example, with $c = \lambda = 1/2$ and an even d_1 we can consider, in addition to φ_u , the mirror map: $\varphi_m(j) := d_1 - j + 1$. It is easy to see that under the conditions of Theorem 2, $P(s_i = j, r_i \leq d_1 - i_\lambda) = 1/d_1$ hence (5) holds and the resulting method, which we refer to as the “mirror method” (because when $L_i = -1$, s_i is the rank symmetrically across the median to r_i), controls the FDR. Similarly, we can choose to use a shift map φ_s : $\varphi_s(j) = j + d_1/2$, which will result in a third FDR-controlling variant of our meta-procedure for $c = \lambda = 1/2$.

Comparing the shift and the mirror maps we note that when $L_i = -1$, φ_s replaces middling target scores with high decoy scores, whereas φ_m replaces low target scores with high decoy scores. Of course, the high decoy scores are the ones more likely to appear in the numerator of (3), and generally we expect the density of the target scores to monotonically decrease with the quality of the score. Taken together, it follows that the estimated FDR will generally be higher when using φ_s than when using φ_m , and hence the variant that uses φ_s will be weaker than the mirror. By extension the randomized φ_u will fall somewhere between the other two maps, as can be partly verified by the comparison of the power using φ_m and φ_u in panel A of Supplementary Figure 2.

We can readily extend the mirroring principle to other values of c and λ where i_c divides $d_1 - i_\lambda$, however when $i_c \nmid d_1 - i_\lambda$ we need to introduce some randomization into the map. Basically, we accomplish this by respecting the mirror principle as much as we can while using the randomization to ensure that (5) holds — hence the name *mirandom* for this map/procedure. It is best described by an example.

Suppose $d = 7$. Then for $i_c = 3$ ($c = 3/8$) and $i_\lambda = 4$ ($\lambda = 1/2$) the mirandom map, φ_{md} , is defined as

$$\varphi_{md}(j) = \begin{cases} 8 & j = 1 \\ 8 \text{ (with probability } 1/3\text{), or } 7 \text{ (with probability } 2/3) & j = 2 \\ 7 \text{ (with probability } 2/3\text{), or } 6 \text{ (with probability } 1/3) & j = 3 \\ 6 & j = 4 \end{cases}$$

Note the uniform coverage ($4/3$) of each value in the range, implying that if j is randomly and uniformly chosen in the domain then $\varphi_{md}(j)$ is uniformly distributed over $\{6, 7, 8\}$.

More generally the mirandom map φ_{md} for a given $c \leq \lambda$ is defined in two steps. In the first step it defines a sequence of $d_1 - i_\lambda$ distributions $F_1, \dots, F_{d_1 - i_\lambda}$ on the range $\{d_1 - i_c + 1, \dots, d_1\}$ so that

- each F_l is defined on a contiguous sequence of natural numbers, and

- if $j < l$ then F_j stochastically dominates F_l and $\min \text{support} \{F_j\} \geq \max \text{support} \{F_l\}$.

In practice, it is straightforward to construct this sequence of distributions and to see that, when combined, they necessarily satisfy the following equal coverage property: for each $j \in \{d_1 - i_c + 1, \dots, d_1\}$, $\sum_{l=1}^{d_1-i\lambda} F_l(j) = \frac{d_1-i\lambda}{i_c}$. In the second step, mirandom defines s_i for any i with $r_i \in \{1, \dots, d_1 - i_c\}$ by randomly drawing a number from F_{r_i} (independently of everything else).

It follows from the equal coverage property that for any $i \in N$ and $j \in \{d_1 - i_c + 1, \dots, d_1\}$ (5) holds for φ_{md} for essentially the same reason it held for φ_u in (6). Hence, the mirandom map allows us to control the FDR for any pre-determined values of c, λ .

3.6 Data-driven setting of the tuning parameters c, λ : finite-decoy Storey (FDS)

All the procedures we consider henceforth are based on the mirandom map. Where they differ is in how they set c, λ .

For example, choosing $c = \lambda = 1/2$ gives us the mirror (assuming d_1 is even), $c = \lambda = 1/d_1$ yields the max, while choosing $\lambda = 1/2$ and $c = \alpha \leq 1/2$ coincides with Lei and Fithian’s recommendation in the related context of sequential hypothesis testing (technically we set $c = \lfloor \alpha \cdot d_1 \rfloor / d_1$ and refer to this method as “LF”). All of these seem plausible; however, our extensive simulations (Supplementary Section 6.2) show that none dominates the others with substantial power to be gained/lost for any particular problem (Supplementary Figure 2, panels B-D).

As the optimal values of c, λ seem to vary in a non-trivial way with the nature of the data, as well as with d and α , we turned to data-driven approaches to setting c, λ .

Lei and Fithian pointed out the connection between the (c, λ) parameters of their AS procedure (they refer to c as s) and the corresponding parameters in Storey’s procedure. Specifically, AS’s λ is analogous to the parameter λ of Storey, Taylor, and Siegmund (2004) that determines the interval $(\lambda, 1]$ from which π_0 , the fraction of true null hypotheses is estimated. Specifically, in the finite sample case, π_0 is estimated as:

$$\hat{\pi}_0^*(\lambda) = \frac{m - R(\lambda) + 1}{(1 - \lambda)m}, \quad (7)$$

where m is again the number of hypotheses, and $R(\lambda)$ is the number of discoveries at threshold λ (number of hypotheses whose p-value is $\leq \lambda$). The c parameter is analogous to the threshold

$$t_\alpha \left(\widehat{\text{FDR}}_\lambda^* \right) = \sup \left\{ t \in [0, 1] : \widehat{\text{FDR}}_\lambda^* \leq \alpha \right\} \quad (8)$$

of Storey et al. (2004), where

$$\widehat{\text{FDR}}_\lambda^* = \begin{cases} \frac{m \cdot \hat{\pi}_0^*(\lambda) \cdot t}{R(t) \vee 1} & t \leq \lambda \\ 1 & t > \lambda \end{cases}. \quad (9)$$

We take this analogy one step further and essentially use the procedure of Storey et al. (2004) to determine c by applying it to the empirical p-values, $\tilde{p}_i := (d_1 - r_i + 1)/d_1$. However, to do that, we first need to determine λ .

We could have determined λ by applying the bootstrap approach of Storey et al. (2004) to \tilde{p}_i . However, in practice we found that using the bootstrap option of the qvalue package (Storey et al., 2019) in our setup can significantly compromise our FDR control. Therefore, instead we devised an alternative approach inspired by the spline-based method of Storey and Tibshirani (2003) for estimating π_0 , where we look for the flattening of the tail of the p-value histogram as we approach

1. Because our p-values, \tilde{p}_i , lie on the lattice i/d_1 for $i = 1, \dots, d_1$, instead of threading a spline as in Storey and Tibshirani (2003), we repeatedly test whether the number of p-values in the first half of the considered tail interval $(\lambda, 1]$ is significantly larger than their number in the second half of this interval (Supplementary Section 6.3).

Our finite-decoy Storey (FDS) procedure starts with determining λ as above then essentially applies the methodology of Storey et al. (2004) to \tilde{p}_i to set $c = t_\alpha$ before applying mirandom with the chosen c, λ . Specifically, given the FDR threshold $\alpha \in (0, 1)$ and after determining λ FDS proceeds along (7)-(9) using $R(\lambda) = |\{\tilde{p}_i : \tilde{p}_i \leq \lambda\}|$, to determine

$$t_\alpha \left(\widehat{\text{FDR}}_\lambda^* \right) = \max \left\{ i \in \{0, 1, \dots, d_1 \cdot \lambda\} : \frac{m \cdot \hat{\pi}_0^*(\lambda) \cdot i/d_1}{R(i/d_1) \vee 1} \leq \alpha \right\}. \quad (10)$$

This in principle is our threshold c except that, especially when d is small, $t_\alpha \left(\widehat{\text{FDR}}_\lambda^* \right)$ can often be zero which is not a valid value for c in our setup. Hence FDS defines

$$c := \max \left\{ 1/d_1, t_\alpha \left(\widehat{\text{FDR}}_\lambda^* \right) \right\}. \quad (11)$$

With (c, λ) determined, FDS continues by applying the mirandom procedure with the chosen parameter values.

FDS was defined as close as possible to Storey et al. (2004)'s recommended procedure for guaranteed FDR control in the finite setting (albeit with a pre-determined λ). Indeed, as we argue in Supplementary Section 6.4, FDS converges to a variant of Storey's procedure once we let $d \rightarrow \infty$ (the mirror and mirandom maps in general have an interesting limit in that setup). However, we found that the following variant of FDS that we denote as FDS_1 , often yields better power in our setting, so we considered both variants. FDS_1 differs from FDS as follows:

- When computing $t_\alpha \left(\widehat{\text{FDR}}_\lambda^* \right)$ (10) we use Storey's large sample formulation which does not include the $+1$ in the estimator $\hat{\pi}_0^*(\lambda)$ (7), and maximizes over $i \in \{0, 1, \dots, d_1\}$.
- Instead of defining c as in (11), FDS_1 defines $c := \min \left\{ c_{\max}, 1/d_1 + t_\alpha \left(\widehat{\text{FDR}}_\lambda^* \right) \right\}$, where c_{\max} is some hard bound on c (we used $c_{\max} = 0.95$).
- With FDS_1 's tweaked definition of c the case $c > \lambda$ is now possible. However, mirandom does not allow this so in that case FDS_1 sets $\lambda := c$ instead of the value of λ defined above.

FDS and FDS_1 peek at the data to set c, λ hence they no longer fall under mirandom's guaranteed FDR control and we resorted to empirically examining their FDR control. Specifically, we applied each method to 10K randomly drawn datasets for each of 1200 different combinations of parameter values spanning a wide range of the parameter space (Supplementary Section 6.2). The 1200 combinations were evenly split between calibrated and non-calibrated scores and the empirical FDR of a method at a selected FDR threshold α is the 10K-sample average of the FDP of the method's discovery list at α .

As can be seen in panels A-C of Supplementary Figure 3 the empirical violations of FDR control of FDS and FDS_1 are roughly in line with that of the max method. Specifically, the overall maximal observed violation is 5.0% for FDS, FDS_1 while it is 6.7% for max. Similarly, the number of curves (out of 1200) in which the maximal violation exceeds 2% is 7 for FDS and FDS_1 , and 24 for the

max. Given that the max provably controls the FDR these simulations suggest that FDS and FDS₁ essentially control the FDR as well.

In terms of power FDS₁ seems to deliver overall more power than the mirror, max, LF, FDS and TDC, and often substantially more (Supplementary Figure 4, panels A-E). We note, however, that at times FDS₁ has 10-20% less power than the optimal method, and we observed an even more extreme loss of power with the examples mentioned in Supplementary Section 6.1 where BH has no power (Supplementary Section 6.7). These issues motivate our next procedure.

3.7 A bootstrap procedure for selecting an optimal method

Our final, and ultimately our recommended multi-decoy procedure, uses a novel resampling approach to choose the optimal procedure among several of the ones we introduced above. Our optimization strategy is indirect: rather than using the resamples to choose the method that maximizes the number of discoveries, we use the resamples to advise us whether or not such a direct maximization approach is likely to control the FDR.

Clearly, a direct maximization would have been ideal had we been able to sample more instances of the data. In reality, that is rarely possible all the more so with our underlying assumption that the decoys are given and that it is forbiddingly expensive to generate additional ones. Hence, when a hypothesis is resampled it comes with its original, as well as its decoy scores, thus further limiting the variability of our resamples. In particular, direct maximization will occasionally fail to control the FDR. Our Labeled Bootstrap monitored Maximization (LBM) procedure tries to identify those cases.

In order to gauge the rate of false discoveries we need labeled samples. To this end, we propose a segmented resampling procedure that makes informed guesses (described below) about which of the hypotheses are false nulls before resampling the indices. The scores $\{\tilde{Z}_i^j\}_{j=0}^d$ associated with each resampled conjectured *true null* index are then randomly permuted, which effectively boils down to randomly sampling $j \in \{0, 1, \dots, d\}$ and swapping the corresponding original score $\tilde{Z}_i^0 = Z_i$ with \tilde{Z}_i^j .

The effectiveness of our resampling scheme hinges on how informed are our guesses of the false nulls. To try and increase the overlap between our guesses and the true false nulls we introduced two modifications to the naive approach of estimating the number of false nulls in our sample and then uniformly drawing that many conjectured false nulls. First, we consider increasing sets of hypotheses $\mathcal{H}_j \subset \mathcal{H}_{j+1}$ and verify that the number of conjectured false nulls we draw from each \mathcal{H}_j agrees with our estimate of the number of false nulls in \mathcal{H}_j . Second, rather than being uniform, our draws within each set \mathcal{H}_j are weighted according to the empirical p-values so that hypotheses with more significant empirical p-values are more likely to be drawn as conjectured false nulls. Our segmented resampling procedure is described in detail in Supplementary Section 6.5.

In summary, LBM relies on the labeled resamples of our segmented resampling approach to estimate whether we are likely to control the FDR when using direct maximization (we chose FDS, mirror, and FDS₁ as the candidate methods). If so, then LBM uses the maximizing method; otherwise, LBM chooses a pre-determined fall-back method (here we consistently use FDS₁). Further details are provided in Supplementary Section 6.6.

Our simulations suggest that LBM's control of the FDR is on-par with that of the, provably FDR-controlling, max: the overall maximal observed violation is 5.0% for LBM while it is 6.7% for max,

and the number of curves (out of 1200) in which the maximal violation exceeds 2% is 21 for LBM, and 24 for the max (panels A and D, Supplementary Figure 3). Power-wise LBM arguably offers the best balance among our proposed procedures, offering substantially more power in many of the experiments while never giving up too much power when it is not optimal (Supplementary Figure 5). Finally, going back to the examples mentioned in Supplementary Section 6.1 we find that all our methods, including LBM, essentially control the FDR where Storey’s procedure substantially failed to do so, and similarly that LBM delivers substantial power where BH had none (Supplementary Section 6.7).

4 The peptide detection problem

Our peptide detection procedure starts with a generalization of the WOTE procedure of Granholm et al. (2013). We use Tide (Diament and Noble, 2011) to find for each spectrum its best matching peptide in the target database as well as in the d decoy peptide databases. We then assign to the i th target peptide the observed score, Z_i , which is the maximum of all the PSM scores that were optimally matched to this peptide. We similarly define the maximal scores of each of that peptide’s d randomly shuffled copies as the corresponding decoy scores: $\tilde{Z}_i^1, \dots, \tilde{Z}_i^d$. If no spectrum was optimally matched to a peptide then that peptide’s score is $-\infty$.

We then applied to the above scores TDC ($d = 1$, with the +1 finite sample correction) — representing a peptide-level analogue of the picked target-decoy strategy of Savitski et al. (2015) — as well as the mirror, LBM and the averaging-based aTDC¹ each using $d \in \{3, 5, 7, 9\}$.

Clearly, the competition-based control of the FDR is subject to the variability of the drawn competing scores. To ameliorate the effect of decoy-induced variability on our comparative analysis we report the average of our analysis over 100 applications of each method using that many randomly drawn decoy sets (Supplementary Section 6.8).

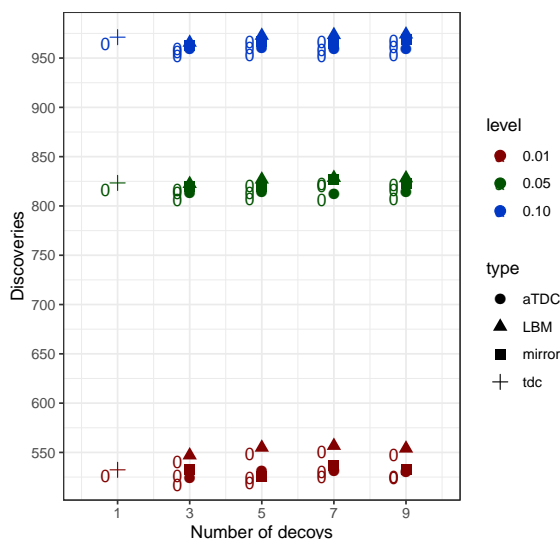
We applied our analysis to three datasets: “human”, “yeast” and “ISB18”² (Supplementary Section 6.8), and examined both the power of the considered methods (in all three datasets) and the FDR control (only in ISB18, as explained in Supplementary Section 6.8). Panel D of Figure 1 suggests that when applied to the ISB18 dataset all our procedures seem to control the FDR: the empirically estimated FDR is always below the selected threshold. In terms of power, again we see that LBM is the overall winner: it typically delivers the largest number of discoveries, and even in the couple of cases where it fails to do so it is only marginally behind the top method (panels A–C). In contrast, each of the other methods has some cases where it delivers noticeably fewer discoveries. In practice, this means that scientists can extract more useful information (discoveries) from the same wet lab experiment by leveraging more computational power coupled with LBM.

More specifically, for $\alpha = 0.01$ LBM’s average of 142.0 ISB18 discoveries ($d = 3$) represents an 8.0% increase over TDC’s average of 131.5 ISB18 discoveries, and we see a 9.4% increase over TDC when using $d = 5$ (143.3 discoveries). In the human dataset and for the same $\alpha = 0.01$ we see a 2.8% increase in power going from TDC to LBM with $d = 3$ (532.4 vs. 547.1 discoveries), and a 4.2% increase when using LBM with $d = 5$ (555.0 discoveries). LBM offers the biggest gains in the yeast dataset where we see (again $\alpha = 0.01$) a 45.5% increase in power going from TDC to LBM

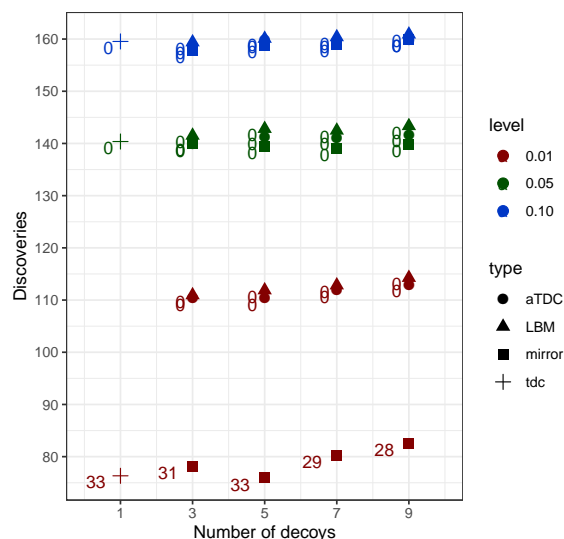
¹We used the version named aTDC₁⁺, which was empirically shown to control the FDR even for small thresholds / datasets (Keich et al., 2018).

²In the case of the ISB18 the data consists of 9 aliquots or replicates, so our analysis was separately applied to each aliquot and then averaged over the aliquots.

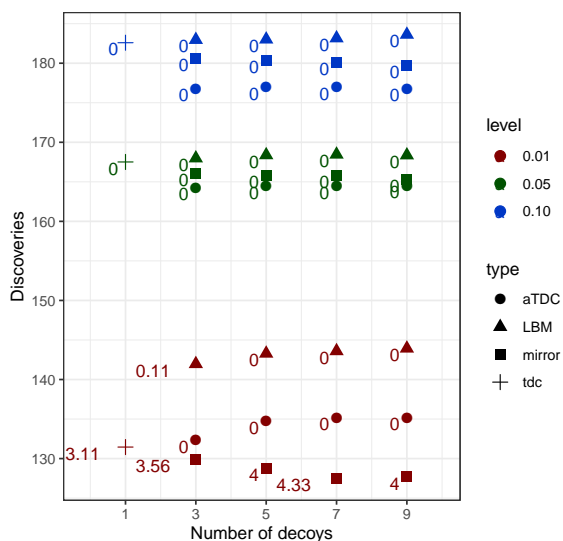
A: human



B: yeast



C: ISB18 (power)



D: ISB18 (FDR control)

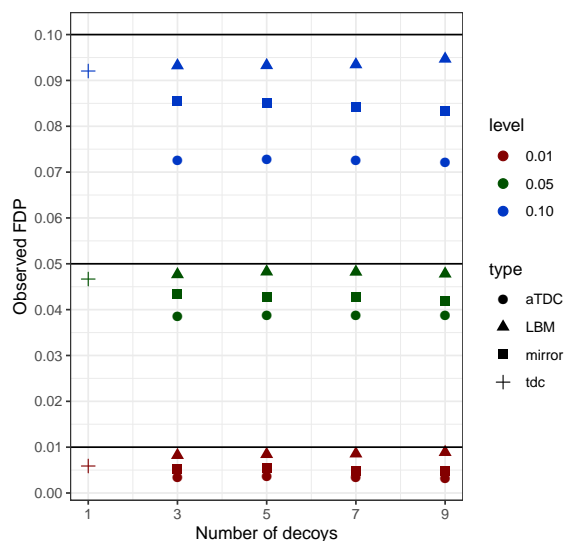


Figure 1: **Peptide detection.** (A: human) The number of discoveries at the given FDR threshold is the average over the 100 randomly drawn decoys sets. Specifically, for each $d \in \{1, 3, 5, 7, 9\}$ we randomly drew 100 decoys sets, each with exactly d decoys, and applied TDC ($d = 1$), the mirror, LBM and aTDC ($d \in \{3, 5, 7, 9\}$) to the target and the drawn set of d decoy scores. We then noted the number of target discoveries at FDR thresholds of 1%, 5% and 10%, and finally we averaged those numbers over the 100 drawn decoy sets. The numbers to the left of the markers indicate the number of runs (out of 100) in which no discovery was reported. (B: yeast) Same as (A) but for the yeast dataset. (C: ISB18, power) Similar to (A) and (B) except for the ISB18 where the data consists of 9 aliquots or replicates. Therefore, the number of discoveries is averaged over the 9 aliquots, where for each aliquot we averaged the number of discoveries over 100 randomly drawn sets of d decoys as explained above. The numbers to the left of the marker indicate the aliquots-average number of runs (out of 100) in which no discovery was reported. (D: ISB18, FDR) Similar to (C) only here we noted the putative FDP of each run (as explained in Supplementary Section 6.8), then we averaged the FDP across the 100 runs to get an empirical FDR for each aliquot that we then averaged over the aliquots. Notably, in all cases the empirical FDR was lower than the selected threshold.

with $d = 3$ (76.3 vs. 111.0 discoveries), and a 46.7% increase when using LBM with $d = 5$ (111.9 discoveries). Moreover, we note that for this $\alpha = 0.01$ TDC reported 0 yeast discoveries in 33 of the 100 runs (each using a different decoy database), whereas LBM reported a positive number of discoveries in all 100 runs for each $d > 1$ we considered.

At the higher FDR thresholds of 0.05 and 0.1 LBM offers a much smaller power advantage over TDC and is marginally behind for $\alpha = 0.1$ and $d = 3$ in the human and yeast datasets. Also, consistent with our simulations, we find that the mirror lags behind LBM, and in fact in these real datasets it is roughly on par with TDC.

To better understand the practical advantage offered by LBM, we focused on a particular case: analysis of the yeast data set using an FDR threshold of $\alpha = 0.01$. The goal of many proteomics experiments is to understand what biological pathways are active in a given sample. We note that, as reported above, when using a single run of the yeast data for 33 of the 100 decoy databases we drew, TDC found 0 discoveries at this 1% FDR threshold meaning that in 1/3 of similarly conducted experiments we would not be able to draw any conclusion using this threshold. As noted above, LBM always reports some discoveries when analyzing the same spectra set at 1% FDR.

We next added two more spectra runs to the yeast dataset (Supplementary Section 6.8) representing a higher budget experiment. In this case at 1% FDR the average number of TDC discoveries was 275.9 and for LBM using $d = 5$ decoys it was 294. Accordingly, we focused on two sets of reported peptides, one of 294 peptides detected by LBM (with $d = 5$) and another of 276 peptides detected via TDC. We eliminated from each group peptides that occur in more than one protein, and then subjected the remaining 54 and 50 proteins, respectively, to analysis via the PANTHER Classification System (<http://pantherdb.org>) (Mi et al., 2013). Specifically, we performed an overrepresentation test for Gene Ontology biological process terms relative to the whole genome background. We used the “slim” term set and Fisher’s exact test, controlling FDR via BH at 5%. This process yields 15 significantly overrepresented biological process terms from the TDC list and 17 from the LBM list (Table 1). The two missing terms—“cellular protein localization” and “cellular macromolecule localization”—are closely related and imply that the sample under investigation is enriched for proteins responsible in shuttling or maintaining other proteins in their proper cellular compartments. Critically, an analysis based solely on the traditional TDC approach would entirely miss this property of the sample being analyzed.

Finally, although aTDC was designed for the spectrum identification problem and in practice was never applied to the peptide detection problem, it was instructive to add aTDC to this comparison. LBM consistently delivered more detected peptides than aTDC did, although in some cases the difference is marginal. Still, in the human dataset for $\alpha = 0.01$ with $d = 3$ we see a 4.4% increase in power going from aTDC to LBM (524.2 vs. 547.1 discoveries), and with $d = 5$ a 4.6% increase when using LBM (530.8 vs. 555.0 discoveries). Similarly, in the ISB18 dataset for $\alpha = 0.01$ with $d = 3$ we see a 7.3% increase in power going from aTDC to LBM (132.3 vs. 142.0 discoveries), and with $d = 5$ a 6.4% increase when using LBM (134.7 vs. 143.3 discoveries).

5 Discussion

We consider a new perspective on the peptide detection problem, which can be framed more broadly as multiple-competition based FDR control. The problem we pose and the tools we offer can be viewed as bridging the gap between the canonical FDR controlling procedures of BH and Storey and the single-decoy approach of the popular TDC used in spectrum identification (ID). Indeed, our

Gene Ontology term	TDC q -value	LBM q -value
cellular response to unfolded protein (GO:0034620)	9.35E-05	1.41E-04
response to unfolded protein (GO:0006986)	7.79E-05	1.18E-04
chaperone-mediated protein folding (GO:0061077)	1.37E-04	2.07E-04
cellular response to heat (GO:0034605)	1.83E-04	2.77E-04
response to heat (GO:0009408)	1.99E-04	3.00E-04
response to topologically incorrect protein (GO:0035966)	3.11E-04	4.68E-04
tRNA metabolic process (GO:0006399)	2.42E-02	3.31E-02
response to stress (GO:0006950)	7.73E-03	1.15E-02
cellular amino acid metabolic process (GO:0006520)	1.14E-02	1.68E-02
protein folding (GO:0006457)	1.31E-02	1.93E-02
translation (GO:0006412)	9.74E-07	2.94E-06
formation of translation initiation ternary complex (GO:0001677)	1.37E-05	3.38E-05
translational termination (GO:0006415)	9.10E-06	2.26E-05
translational elongation (GO:0006414)	6.83E-06	1.69E-05
cellular protein localization (GO:0034613)	—	2.93E-02
cellular macromolecule localization (GO:0070727)	—	3.13E-02
gene expression (GO:0010467)	2.47E-02	4.77E-02

Table 1: **Statistical overrepresentation of Gene Ontology terms in the yeast data set.** Each row is a Gene Ontology biological process term that is deemed significant at $FDR < 0.05$. Enrichments were tested twice, with respect to peptides identified using TDC and LBM.

proposed FDS converges to Storey’s method as the number of decoys $d \rightarrow \infty$ (Supplementary Section 6.4).

The methods we propose here rely on our novel mirandom procedure, which guarantees FDR control in the finite sample case for any pre-determined values of the tuning parameters c, λ . Our extensive simulations show that which of our methods delivers the maximal power varies with the properties of the experiment, as well as with the FDR threshold α . This variation motivates our introduction of LBM. LBM relies on a novel labeled resampling technique, which allows it to select its preferred method after testing whether a direct maximization approach seems to control the FDR. Our simulations suggest that LBM largely controls the FDR and seems to offer the best balance among our multi-decoy methods as well as a significant power advantage over the single-decoy TDC.

Applying our methods to the peptide detection problem suggests that, as with the simulated data, the FDR is controlled and LBM can deliver significantly more power (up to almost 50% more discoveries) than the single decoy TDC.

We stress that the problem of peptide detection is important not only as a stepping stone toward the downstream goal of detecting proteins; in many proteomics studies, the peptides themselves are of primary interest. For example, MS/MS is being increasingly applied to complex samples, ranging from the microbiome in the human gut (Lin et al., 2019) to microbial communities in environmental samples such as soil or ocean water (Saito et al., 2019). In these settings, the genome sequences of the species in the community are only partially characterized, so protein inference is problematic. Nonetheless, observation of a particular peptide can often be used to infer the presence of a group of closely related species (a taxonomic clade) or closely related proteins (a homology group).

Peptide detection is also of primary interest in studies that aim to detect so-called “proteoforms” — variants of the same protein that arise due to differential splicing of the mature RNA or due to post-translational modifications of the translated protein. Identifying proteoforms can be critically important, for example, in the study of diseases like Alzheimer’s or Parkinson’s disease, in which the disease is hypothesized to arise in part due to the presence of deviant proteoforms (Morris et al., 2015; Ping et al., 2018; Wildburger et al., 2017).

Finally, as mentioned in the Introduction, our approach is applicable beyond peptide detection. Moreover, while we stated our results assuming iid decoys, the results hold in a more general setting of “*conditional null exchangeability*” (Supplementary Section 6.9). This exchangeability is particularly relevant for future work on generalizing the construction of Barber and Candès (2015) to multiple knockoffs, where the iid decoys assumption is unlikely to hold.

Related work. We recently developed aTDC in the context of spectrum ID. The goal of aTDC was to reduce the decoy-induced variability associated with TDC by averaging a number of single-decoy competitions (Keich and Noble, 2017b; Keich et al., 2018). As such, aTDC fundamentally differs from the methods of this paper which simultaneously use all the decoys in a single competition; hence, the methods proposed here can deliver a significant power advantage over aTDC (panel F, Supplementary Figure 5 and Supplementary Figure 1). Our new methods are designed for the iid (or exchangeable) decoys case, which is a reasonable assumption for the peptide detection problem studied here but does not hold for the spectrum ID for which aTDC was devised. Indeed, as pointed out in Keich and Noble (2017a), due to the different nature of native/foreign false discoveries, the spectrum ID problem fundamentally differs from the setup of this paper and even the above, weaker, null exchangeability property does not hold in this case. Thus, LBM cannot replace aTDC entirely; indeed, LBM is too liberal in the context of the spectrum ID problem. Note that in practice aTDC has not previously been applied to the peptide detection problem.

While working on this manuscript we became aware of a related Arxiv submission (He et al., 2018). The initial version of that paper had just the mirror method, which as we show is quite limited in power. A later version that essentially showed up simultaneously with the submission of our technical report (Emery et al., 2019) extended their approach to a more general case; however, the method still consists of a subset of our independently developed research in that: (a) they do not consider the λ tuning parameter, (b) they use the uniform random map φ_u which, as we show, is inferior to mirandom, and (c) they do not offer either a general deterministic (FDS) or bootstrap based (LBM) data-driven selection of the tuning parameter(s), relying instead on a method that works only in the limited case-control scenario they consider.

References

- R. F. Barber and Emmanuel J. Candès. Controlling the false discovery rate via knockoffs. *The Annals of Statistics*, 43(5): 2055–2085, 2015.
- Y. Benjamini and Y. Hochberg. Controlling the false discovery rate: a practical and powerful approach to multiple testing. *Journal of the Royal Statistical Society Series B*, 57:289–300, 1995.
- Y. Benjamini and Y. Hochberg. On the adaptive control of the false discovery rate in multiple testing with independent statistics. *Journal of Educational Behavioral Statistics*, 25(60–83), 2000.
- Y. Benjamini, A. M. Krieger, and D. Yekutieli. Adaptive linear step-up procedures that control the false discovery rate. *Biometrika*, 93(3):491–507, 2006.

- F. R. Cerqueira, A. Graber, B. Schwikowski, and C. Baumgartner. MUDE: a new approach for optimizing sensitivity in the target-decoy search strategy for large-scale peptide/protein identification. *Journal of Proteome Research*, 9(5): 2265–2277, 2010.
- B. Diament and W. S. Noble. Faster SEQUEST searching for peptide identification from tandem mass spectra. *Journal of Proteome Research*, 10(9):3871–3879, 2011.
- J. E. Elias and S. P. Gygi. Target-decoy search strategy for increased confidence in large-scale protein identifications by mass spectrometry. *Nature Methods*, 4(3):207–214, 2007.
- J. E. Elias and S. P. Gygi. Target-decoy search strategy for mass spectrometry-based proteomics. *Methods in Molecular Biology*, 604(55–71), 2010.
- K. Emery, S. Hasam, W. S. Noble, and U. Keich. Multiple competition based fdr control. *arXiv preprint arXiv:1907.01458*, 2019.
- J. K. Eng, A. L. McCormack, and J. R. Yates, III. An approach to correlate tandem mass spectral data of peptides with amino acid sequences in a protein database. *Journal of the American Society for Mass Spectrometry*, 5:976–989, 1994.
- Yingying Fan, Jinchi Lv, Mahrad Sharifvaghefi, and Yoshimasa Uematsu. IPAD: stable interpretable forecasting with knockoffs inference. *Available at SSRN 3245137*, 2018.
- Chao Gao, Hanbo Sun, Tuo Wang, Ming Tang, Nicolaas I Bohnen, Martijn LTM Müller, Talia Herman, Nir Giladi, Alexandr Kalinin, Cathie Spino, et al. Model-based and model-free machine learning techniques for diagnostic prediction and classification of clinical outcomes in parkinsons disease. *Scientific Reports*, 8(1):7129, 2018.
- V. Granholm, J. F. Navarro, W. S. Noble, and L. Käll. Determining the calibration of confidence estimation procedures for unique peptides in shotgun proteomics. *Journal of Proteomics*, 80(27):123–131, 2013.
- C. T. Harbison, D. B. Gordon, T. I. Lee, N. Rinaldi, K. D. Macisaac, T. D. Danford, N. M. Hannett, J. Tagne, D. B. Reynolds, J. Yoo, E.G. Jennings, J. Zeitlinger, D.K. Pokholok, M. Kellis, P. A. Rolfe, K. T. Takusagawa, E. S. Lander, D. K. Gifford, E. Fraenkel, and R. A. Young. Transcriptional regulatory code of a eukaryotic genome. *Nature*, 431: 99–104, 2004.
- K. He, Y. Fu, W.-F. Zeng, L. Luo, H. Chi, C. Liu, L.-Y. Qing, R.-X. Sun, and S.-M. He. A theoretical foundation of the target-decoy search strategy for false discovery rate control in proteomics. *arXiv*, 2015. URL <https://arxiv.org/abs/1501.00537>.
- K. He, M. Li, Y. Fu, F. Gong, and X. Sun. A direct approach to false discovery rates by decoy permutations. *arXiv preprint arXiv:1804.08222*, 2018.
- K. Jeong, S. Kim, and N. Bandeira. False discovery rates in spectral identification. *BMC Bioinformatics*, 13(Suppl. 16): S2, 2012.
- U. Keich and W. S. Noble. On the importance of well calibrated scores for identifying shotgun proteomics spectra. *Journal of Proteome Research*, 14(2):1147–1160, 2015.
- U. Keich and W. S. Noble. Controlling the FDR in imperfect database matches applied to tandem mass spectrum identification. *Journal of the American Statistical Association*, 2017a. <https://doi.org/10.1080/01621459.2017.1375931>.
- U. Keich and W. S. Noble. Progressive calibration and averaging for tandem mass spectrometry statistical confidence estimation: Why settle for a single decoy. In S. Sahinalp, editor, *Proceedings of the International Conference on Research in Computational Biology (RECOMB)*, volume 10229 of *Lecture Notes in Computer Science*, pages 99–116. Springer, 2017b.
- U. Keich, A. Kertesz-Farkas, and W. S. Noble. Improved false discovery rate estimation procedure for shotgun proteomics. *Journal of Proteome Research*, 14(8):3148–3161, 2015.

- U. Keich, K. Tamura, and W. S. Noble. Averaging strategy to reduce variability in target-decoy estimates of false discovery rate. *Journal of Proteome Research*, 18(2):585–593, 2018.
- J. Klimek, J. S. Eddes, L. Hohmann, J. Jackson, A. Peterson, S. Letarte, P. R. Gafken, J. E. Katz, P. Mallick, H. Lee, A. Schmidt, R. Ossola, J. K. Eng, R. Aebersold, and D. B. Martin. The standard protein mix database: a diverse data set to assist in the production of improved peptide and protein identification software tools. *Journal of Proteome Research*, 7(1):96–1003, 2008.
- L. Lei and W. Fithian. Power of ordered hypothesis testing. In *International Conference on Machine Learning*, pages 2924–2932, 2016.
- L. I. Levitsky, M. V. Ivanov, A. A. Lobas, and M. V. Gorshkov. Unbiased false discovery rate estimation for shotgun proteomics based on the target-decoy approach. *Journal of Proteome Research*, 16(2):393–397, 2017.
- H. Lin, Q. Y. He, L. Shi, M. Sleeman, M. S. Baker, and E. C. Nice. Proteomics and the microbiome: pitfalls and potential. *Expert Reviews in Proteomics*, 16(6):501–511, 2019.
- Y. Y. Lu, Y. Fan, J. Lv, and W. S. Noble. DeepPINK: reproducible feature selection in deep neural networks. In *Advances in Neural Information Processing Systems*, 2018.
- D. H. May, K. Tamura, and W. S. Noble. Param-Medic: A tool for improving MS/MS database search yield by optimizing parameter settings. *Journal of Proteome Research*, 16(4):1817–1824, 2017.
- H. Mi, A. Muruganujan, and P. T. Thomas. PANTHER in 2013: modeling the evolution of gene function, and other gene attributes, in the context of phylogenetic trees. *Nucleic Acids Research*, 41(Database issue):D377–D386, 2013.
- M. Morris, G. M. Knudsen, S. Maeda, J. C. Trinidad, A. Ioanoviciu, A. L. Burlingame, and L. Mucke. Tau post-translational modifications in wild-type and human amyloid precursor protein transgenic mice. *Nature Neuroscience*, 18:1183–1189, 2015.
- A. I. Nesvizhskii. A survey of computational methods and error rate estimation procedures for peptide and protein identification in shotgun proteomics. *Journal of Proteomics*, 73(11):2092 – 2123, 2010.
- P. Ng and U. Keich. Gimsan: a gibbs motif finder with significance analysis. *Bioinformatics*, 24(19):2256–2257, 2008.
- W. S. Noble and M. J. MacCoss. Computational and statistical analysis of protein mass spectrometry data. *PLOS Computational Biology*, 8(1):e1002296, 2012.
- M. Muller P. Hernandez and R. D. Appel. Automated protein identification by tandem mass spectrometry: Issues and strategies. *Mass Spectrometry Reviews*, 25:235–254, 2006.
- C. Y. Park, A. A. Klammer, L. Käll, M. P. MacCoss, and W. S. Noble. Rapid and accurate peptide identification from tandem mass spectra. *Journal of Proteome Research*, 7(7):3022–3027, 2008.
- L. Ping, D. M. Duong, L. Yin, M. Gearing, J. J. Lah, A. I. Levey, and N. T. Seyfried. Global quantitative analysis of the human brain proteome in Alzheimers and Parkinsons disease. *Scientific Data*, 5:180036, 2018.
- D. F. Read, K. Cook, Y. Y. Lu, K. Le Roch, and W. S. Noble. Predicting gene expression in the human malaria parasite *plasmodium falciparum*. *Journal of Proteome Research*, 2019. In press.
- M. A. Saito, E. M. Bertrand, M. E. Duffy, D. A. Gaylord, N. A. Held, W. J. Hervey, R. L. Hettich, P. D. Jagtap, M. G. Janech, D. B. Kinkade, D. H. Leary, M. R. McIlvin, E. K. Moore, R. M. Morris, B. A. Neely, B. L. Nunn, J. K. Saunders, A. I. Shepherd, N. I. Symmonds, and D. A. Walsh. Progress and challenges in ocean metaproteomics and proposed best practices for data sharing. *Journal of Proteome Research*, 18(4):1461–1476, 2019.
- M. M. Savitski, M. Wilhelm, H. Hahne, B. Kuster, and M. Bantscheff. A scalable approach for protein false discovery rate estimation in large proteomic data sets. *Molecular & Cellular Proteomics*, 14(9):2394–2404, 2015.

- M. Schittmayer, K. Fritz, L. Liesinger, J. Griss, and R. Birner-Gruenberger. Cleaning out the litterbox of proteomic scientists' favorite pet: Optimized data analysis avoiding trypsin artifacts. *Journal of Proteome Research*, 15(4): 1222–1229, 2016.
- J. D. Storey. A direct approach to false discovery rates. *Journal of the Royal Statistical Society Series B*, 64:479–498, 2002.
- J. D. Storey and R. Tibshirani. Statistical significance for genome-wide studies. *Proceedings of the National Academy of Sciences of the United States of America*, 100:9440–9445, 2003.
- J. D. Storey, J. E. Taylor, and D. Siegmund. Strong control, conservative point estimation, and simultaneous conservative consistency of false discovery rates: A unified approach. *Journal of the Royal Statistical Society, Series B*, 66:187–205, 2004.
- John D. Storey, Andrew J. Bass, Alan Dabney, and David Robinson. *qvalue: Q-value estimation for false discovery rate control*, 2019. URL <http://github.com/jdstorey/qvalue>. R package version 2.14.1.
- V. G. Tusher, R. Tibshirani, and G. Chu. Significance analysis of microarrays applied to the ionizing radiation response. *Proceedings of the National Academy of Sciences of the United States of America*, 98:5116–5121, April 2001. ISSN 0027-8424. doi: 10.1073/pnas.091062498.
- N. C. Wildburger, T. J. Esparza, R. D. LeDuc, R. T. Fellers, P. M. Thomas, N. J. Cairns, N. L. Kelleher, R. J. Bateman, and D. L. Brody. Diversity of amyloid-beta proteoforms in the Alzheimers disease brain. *Scientific Reports*, 7:9520, 2017.
- F. Xia, M. J. Zhang, J. Y. Zou, and D. Tse. NeuralFDR: Learning discovery thresholds from hypothesis features. In *Advances in Neural Information Processing Systems*, pages 1541–1550, 2017.
- Y. Xiao, M. T. Angulo, J. Friedman, M. K. Waldor, S. T. WeissT, and Y.-Y. Liu. Mapping the ecological networks of microbial communities. *Nature Communications*, 8(1):2042, 2017.
- L. Zhong, J. Zhou, X. Chen, Y. Lou, D. Liu, X. Zou, B. Yang, Y. Yin, and Y. Pan. Quantitative proteomics study of the neuroprotective effects of B12 on hydrogen peroxide-induced apoptosis in SH-SY5Y cells. *Scientific Reports*, 6: 22635, 2016.

6 Supplementary Material

6.1 The problem with pooling the decoys

Two significant problems arise when pooling the decoys to compute the p-values. First, these p-values do not satisfy the assumption that the p-values of the true null hypotheses are independent: because all p-values are computed using the same batch of pooled decoy scores, it is clear that they are dependent to some extent. While this dependency diminishes as $m \rightarrow \infty$, there is a second, more serious problem that in general cannot be alleviated by considering a large enough m .

Specifically, in pooling the decoys we make the implicit assumption that the score is calibrated, i.e., that all true null scores are generated according to the same distribution. If this assumption is violated, as is typically the case in the spectrum identification problem for one (Keich and Noble, 2015), then the p-values of the true null hypotheses are not identically distributed, and in particular they are also not (discrete) uniform in general. This means that even the more conservative BH procedure is no longer guaranteed to control the FDR, and the problem is much worse with Storey. Indeed, Supplementary Section 6.1.1 below shows that there are arbitrary large examples wherein Storey significantly fails to control the FDR, and similar ones where BH is essentially powerless. Those examples, demonstrate that, in general, applying BH or Storey's procedure to p-values that are estimated by pooling the competing null scores can be problematic both in terms of power and control of the FDR. Note that these issues have previously been discussed in the context of the spectrum identification problem, where the effect of pooling on power and on FDR control were demonstrated using simulated and real data (Keich and Noble, 2015; Keich, Kertesz-Farkas, and Noble, 2015).

6.1.1 Examples of failings of the canonical procedures

Consider BH applied to just $m = 2$ hypotheses with $d = 1$ decoy, and suppose that $P(\tilde{Z}_1^1 > \tilde{Z}_2^1) = 1$ (i.e., the support of the null distribution corresponding to H_1 is disjoint and to the right of the support of the null distribution corresponding to H_2). Suppose further that both H_i are true nulls, so that the FDR coincides with the FWER (family-wise error rate), which is the probability of at least one (false) discovery. It is easy to see that in this case using the FDR threshold $\alpha := 2/3$ the event $\{Z_1 > \tilde{Z}_1^1, Z_2 < \tilde{Z}_2^1\}$ will produce one discovery ($p_1 := \text{p-value}(Z_1) = 1/3, p_2 := \text{p-value}(Z_2) = 1$), and the disjoint event $\{Z_2 > \tilde{Z}_2^1\}$ will produce two discoveries ($p_2 = 2/3$). However, these events have a total probability of $1/4 + 1/2 = 3/4$ so the FWER=FDR is $> \alpha$ in this case.

This effect can be much more pronounced in the case of Storey's method. Suppose that the null hypotheses split into two equal sized groups, A and B , where for every $i \in A$ and $j \in B$, $P(\tilde{Z}_i^1 < \tilde{Z}_j^1) = 1$. Suppose further that all the hypotheses in A are false nulls with scores Z_i satisfying $P(Z_i > \tilde{Z}_i^1) = 1$, and that all hypotheses in B are true nulls. The decoy-pooled p-values will be essentially no greater than $1/2$. Hence, Storey's estimate of π_0 , $\hat{\pi}_0(\lambda) = \frac{m-R(\lambda)}{(1-\lambda)m}$, where m is the number of hypotheses, and $R(\lambda)$ is the number of hypotheses whose p-value is $\leq \lambda$, will significantly underestimate π_0 . For example, if $\lambda \geq 0.5$ then $\hat{\pi}_0 = 0$, which in turn implies that essentially all null hypotheses will be rejected at any FDR level α and particularly for $\alpha < 1/2$,

while the actual FDP will clearly be $1/2$. Even if λ is chosen to better fit these p-values, e.g., $\lambda = 0.25$, or the set-up is changed slightly to allow some group A p-values to be null so $\hat{\pi}_0 \neq 0$, the procedure will still significantly underestimate π_0 and thus underestimate the actual FDR.

Example 1. As a specific example in the above vein we constructed an experiment with $m = 300$ and $d = 5$ decoys where group A 's true null distribution is $N(0, 1)$, and group B 's true null distribution is $N(50, 1)$. We set all 150 hypotheses in group B and 50 of the 150 hypotheses in group A to be true null, and we generated observed scores by sampling from the appropriate null distribution above. We next generated the observed scores for the 100 false null hypotheses in group A by sampling from the same, significantly shifted, $N(50, 1)$ distribution that we used to generate all observed scores of group B . All competing null (decoy) scores were generated using the group's null distribution. In this setup we chose to leave a third of group A as true nulls so that approximately 50 of the p-values will exceed $1/2$ ensuring that $\hat{\pi}_0 > 0$.

We then computed the pooled p-values and applied Storey's FDR controlling procedure, as presented in the package `qvalue` (Storey et al., 2019) (with λ chosen using the `bootstrap` option). This experiment was repeated using 1,000 randomly drawn sets, noting each time the real FDP at FDR thresholds of $\alpha = 0.1$ and $\alpha = 0.2$. As expected in this setting, Storey's procedure clearly failed to control the FDR: at $\alpha = 0.1$, the empirical FDR (the FDP averaged over the 1K samples) was 0.24, or over 200% of what it should be, and for $\alpha = 0.2$ the empirical FDR was larger than 0.5 again indicating a significant violation.

We could not find such examples, with an essentially arbitrary large m and a substantial liberal bias, when using the BH procedure. However, we found a class of arbitrary large examples, similar to the above class (on which Storey fails to control the FDR), where due to pooling the conservative nature of BH was amplified to the point where it was essentially powerless. Consider four groups A, B, C and D and suppose that for every $i \in A, j \in B, k \in C$ and $l \in D$, $P(\tilde{Z}_i^1 < \tilde{Z}_j^1 < \tilde{Z}_k^1 < \tilde{Z}_l^1) = 1$. Suppose further that all the hypotheses in groups A and B are false null with scores that fall in the range of values of the subsequent group, so in particular $P(Z_i > \tilde{Z}_k^1) = 0$ and similarly $P(Z_j > \tilde{Z}_l^1) = 0$. It is easy to see that using pooling in this case the p-values for the (false) null hypotheses in groups A and B will be $\geq 1/2$ and $1/4$ respectively, and it follows that no discoveries can be made by BH with $\alpha < 1/4$, regardless of how large m and d are.

Example 2. Again, we construct a specific example according to the above general outline. We set $m = 300$, so that each of the four groups has 75 hypotheses, and we use $d = 5$ decoys. The null distribution of each group is set as $N(\mu, 1)$, where μ increases from $\mu_A = 0$, by 50, to $\mu_D = 150$. The observed scores corresponding to the 150 false null hypotheses of groups A and B were drawn from the null distributions of group B and C respectively, whereas the 150 observed scores of groups C and D were drawn from their respective null distributions. Using pooled p-values BH does not yield any discovery for any $\alpha \leq 0.65$ amongst any of our 1000 samples, and it was not until using $\alpha = 0.7$ that we finally started seeing some samples on which BH had non-zero power. Incidentally, even using non-pooled p-values is slightly better here: the first samples with non-zero BH power appear for $\alpha = 0.3$.

6.2 Simulation setup

In order to analyze and compare the performance of the FDR-controlling procedures we simulated datasets with both calibrated (all true null scores are generated according to the same distribution) and non-calibrated scores — a comparison that also allowed us to select our overall recommended procedure.

In the non-calibrated case we allow the distribution of the null scores to vary with the hypotheses so we sample from hypothesis-specific distributions. Specifically, for simulating using a non-calibrated score we associate with the null hypothesis H_i a normal $N(\mu_i, \sigma_i^2)$ distribution from which its competing null (decoy/knockoff) scores are sampled. If H_i is labeled a true null, this is also the distribution from which the observed score is sampled. Otherwise, H_i is a false null, so the observed score is sampled from a γ_i -shifted normal $N(\mu_i + \gamma_i, \sigma_i^2)$ distribution, where $\gamma_i > 0$. The parameters μ_i , σ_i^2 , and γ_i are themselves sampled with each newly sampled set of scores:

- μ_i is sampled from a normal $N(\mu, \sigma^2)$ distribution with the hyper-parameters $\mu = 0$ and $\sigma^2 = 1$.
- σ_i^2 is sampled from $1 + \exp(\omega)$, where $\exp(\omega)$ is the exponential distribution with rate $\omega = 1$.
- γ_i is sampled from $1 + \exp(\nu)$, where ν is a hyper-parameter that determines the separation between the false and true null scores

When simulating using a calibrated score the parameters μ_i , σ_i and γ_i are kept constant.

In our non-calibrated score simulations we drew 10K random sets of observed and competing null scores (each with its own randomly drawn values of $\mu_i, \sigma_i, \gamma_i$) for each of the following 600 combinations of parameter (or hyper-parameter) values:

- The number of false null hypotheses, k , was set to each value in $\{1, 10, 10^2, 10^3, 10^4\}$.
- For each value of k , the total number of hypotheses, m , was set to $\min\{c \cdot k, 2 \cdot 10^4\}$ where c was set to each of the following factors $\{1.25, 2, 4, 10, 20, 100, 1000\}$ subject to the constraint that $m \geq 100$.
- For each values of k and m above, the hyper-parameter ν that determines the separation between the false and true null scores was set to each of the values in $\{0.01, 0.05, 0.1, 0.25, 0.5, 1.0\}$.
- For each values of k , m , and ν above, the number of decoys d was set to each of the values in $\{3, 5, 9, 19, 39\}$.

We then used the 10K sampled sets from each of the 600 experiments to find the empirical FDR as well as the power of each method for each selected FDR threshold $\alpha \in \Phi$. For a given threshold α , the power of a method is the average percentage of false nulls that are reported by the method at level α , and the empirical FDR is the average of the FDP in the discovery list (both averages are taken over the experiment's 10K runs). We used a fairly dense set of FDR thresholds Φ : from 0.001 to 0.009 by jumps of 0.001, from 0.01 to 0.29 by jumps of 0.01, and from 0.3 to 0.95 by jumps of 0.05.

Our calibrated score simulation also consisted of 600 experiments, or combinations of parameter values. Specifically, we used the same values of k , m , and d as in the above non-calibrated

simulations and we let γ vary over the values in $\{0.8, 1, 1.4, 2, 3, 4\}$. In each experiment we again draw 10K random sets of observed and competing scores using $\mu_i \equiv 0, \sigma_i \equiv 1, \gamma_i \equiv \gamma$.

In both setups we examined the FDR control by looking at the ratio between the empirical FDR (the observed FDP averaged over 10K runs) and the selected threshold as well as at the power which is the average (over 10K runs) percentage of false nulls we discover.

6.3 Determining λ from the empirical p-values

Given an upper bound Λ on λ (we used 0.95), and a binomial test significance cutoff β (we used 0.1)

1. Initialize: $i := 1$.
2. If $i \geq \Lambda \cdot d_1$ or $i = d$ then
 - set $i_\lambda := i$ and stop.
3. If $i + d_1$ is even then
 - set $i_s := (i + d_1)/2$,
 - $n_p^+ := \# \{\tilde{p}_i \in [(i_s + 1)/d_1, 1]\}$,
 - $n_p^- := \# \{\tilde{p}_i \in [(i + 1)/d_1, i_s/d_1]\}$.
4. Otherwise,
 - set $i_s := (i + d_1 + 1)/2$,
 - $n_p^+ := \# \{\tilde{p}_i \in [(i_s + 1)/d_1, 1]\}$,
 - $n_p^- := \# \{\tilde{p}_i \in [(i + 1)/d_1, (i_s - 1)/d_1]\}$.
5. Calculate $p_b = P(B \geq n_p^-)$ where $B \sim \text{Binomial}(n_p^+ + n_p^-, 0.5)$.
6. If $p_b > \beta$ then (the remaining tail of the p-value histogram “seems to have flattened”)
 - set $i_\lambda := i$ and stop.
7. Otherwise (we are yet to see the flattening of the tail of the p-value histogram),
 - set $i := i + 1$,
 - return to step 2.

Note that the interval $(\lambda, 1]$ from which π_0 is estimated in (7) coincides with $[(i_\lambda + 1)/d_1, 1]$.

6.4 The limiting behavior of our FDR controlling methods

In its selection of the parameter c , FDS essentially applies Storey’s procedure to the empirical p-values; however, there is a more intimate connection between FDS, and more generally between some of the methods described above and Storey’s procedure that becomes clearer once we let $d \rightarrow \infty$. To elucidate that connection we further need to assume here that the score is calibrated, that is, that the distribution of the decoy scores is the same for all null hypotheses. In this case, we

might as well assume our observed scores are already expressed as p-values: $Z_i = p_i$ (keeping in mind that this implies that small scores are better, not worse as they are elsewhere in this paper).

It is not difficult to see that for a given (c, λ) , mirandom assigns, in the limit as $d \rightarrow \infty$, $W_i := Z_i = p_i$ if $p_i \leq c$ ($L_i = 1$, or original win), and $W_i := (1 - p_i) \cdot c / (1 - \lambda) \in [0, c)$ if $p_i > \lambda$ ($L_i = -1$, or decoy win). Sorting the scores W_i in increasing order (smaller scores are better here) $W_{(1)} < W_{(2)} < \dots < W_{(m)}$, we note that for i with $W_{(i)} = p_{(i)} \leq c$ the denominator term $\#\{j \leq i : L_{(j)} = 1\}$ in (3) is the number of original scores, or p-values $p_j \leq p_{(i)}$. At the same time, for the same i and $j \leq i$, $L_{(j)} = -1$ if and only if $p_{(j)} > \lambda$ and $W_{(j)} < W_{(i)} = p_{(i)} \leq c$ so we have for the numerator term

$$\#\{j \leq i : L_{(j)} = -1\} = \#\{j : p_j > \lambda, W_j < p_{(i)}\} = \#\left\{j : p_j > 1 - \frac{1 - \lambda}{c} p_{(i)}\right\}.$$

Considering that $i_{\alpha c \lambda} < m$ in (3) must be attained at an i for which $W_i = p_i \leq c$ (original win), we can essentially rewrite (3) as

$$i_{\alpha c \lambda} = \max \left\{ i : \frac{1 + \#\{j : p_j > 1 - \frac{1 - \lambda}{c} p_{(i)}\}}{\#\{j : p_j \leq p_{(i)}\} \vee 1} \cdot \frac{c}{1 - \lambda} \leq \alpha \right\}. \quad (12)$$

Consider now Storey's selection of the threshold t_α , which when using the more rigorous estimate (7) essentially amounts to

$$t_\alpha = \max \left\{ t \in [0, \lambda^*] : \frac{1 + \#\{j : p_j > \lambda^*\}}{\#\{j : p_j \leq t\} \vee 1} \cdot \frac{t}{1 - \lambda^*} \leq \alpha \right\},$$

where λ^* is a tuning parameter. Considering the cases where $t_\alpha \leq c$ and setting $\lambda^*(t) := 1 - (1 - \lambda)t/c$ Storey's threshold t_α becomes

$$t_\alpha = \max \left\{ t \in [0, c] : \frac{1 + \#\{j : p_j > 1 - \frac{1 - \lambda}{c} t\}}{\#\{j : p_j \leq t\} \vee 1} \cdot \frac{c}{1 - \lambda} \leq \alpha \right\}.$$

Since in practice t_α can be taken as equal to one of the $p_{(i)}$ the equivalence with (12) becomes obvious by identifying t above with $p_{(i)}$ in (12).

Thus, for example, as $d \rightarrow \infty$ the mirror method ($\lambda = c = 1/2$) converges, in the context of a calibrated score, to Storey's procedure using $\lambda^*(t) := 1 - t$, which coincides with the "mirroring method" of Xia et al. (2017). It is worth noting that the general setting $\lambda^*(t) := 1 - (1 - \lambda)t/c$ is not obviously supported by the finite sample theory of Storey et al. (2004); however, it can be justified by noting the above equivalence and our results here.

An even more direct connection with Storey's procedure is established by letting $d \rightarrow \infty$ in the context of FDS. Indeed, using the same λ determined by the progressive interval splitting procedure described in Section 6.3, Storey's finite-sample procedure (8) would amount to setting the rejection threshold to

$$t_\alpha = \max \left\{ t \in [0, \lambda] : \frac{m \cdot \hat{\pi}_0^*(\lambda) \cdot t}{R(t) \vee 1} \leq \alpha \right\}.$$

Recalling that $d_1 \rightarrow \infty$ we note that the latter t_α coincides with the value FDS assigns to c via (10) and (11). Let i_c be such that the above $t_\alpha = c \in [p_{(i_c)}, p_{(i_c+1)})$ (recall we assume no ties here),

then we can assume without loss of generality that $t_\alpha = c = p_{(i_c)}$ and hence (compare with (12)) the mirandom part of FDS will find

$$i_{\alpha c \lambda} = \max \left\{ i \leq i_c : \frac{1 + \#\{j : p_j > 1 - \frac{1-\lambda}{c} p_{(i)}\}}{\#\{j : p_j \leq p_{(i)}\} \vee 1} \cdot \frac{c}{1-\lambda} \leq \alpha \right\}.$$

But

$$\frac{1 + \#\{j : p_j > 1 - \frac{1-\lambda}{c} p_{(i_c)}\}}{\#\{j : p_j \leq p_{(i_c)}\} \vee 1} \cdot \frac{c}{1-\lambda} = \frac{1 + \#\{j : p_j > \lambda\}}{\#\{j : p_j \leq c\} \vee 1} \cdot \frac{c}{1-\lambda} = \frac{m \cdot \hat{\pi}_0^*(\lambda) \cdot t_\alpha}{R(t_\alpha) \vee 1} \leq \alpha.$$

Hence i_c satisfies the required inequality and $i_{\alpha c \lambda} = i_c$. It follows that the rejection lists of FDS and the above variant of Storey's procedure with the same λ coincide in the $d \rightarrow \infty$ limit.

In Supplementary Section 8.7.2 of our technical report Emery et al. (2019) we compare the limiting methods of our procedures as $d \rightarrow \infty$ using the same kind of simulations we use in this paper for the finite decoys case. These experiments showed trends similar to those found in the finite case, indicating that the relationships between the methods continue to the limit.

6.5 Labeled resampling

For clarity of the exposition we break the description of our labeled resampling procedure into two parts with the first describing how we generate a sample of conjectured true/false null labels.

1. Determine λ as described in Supplementary Section 6.3
2. Using $c = \lambda$ from step 1 above, apply steps 1-2 of mirandom (Section 3.2 with $\varphi \equiv \varphi_{md}$ of Section 3.5) to define the assigned scores W_i and labels L_i , and order the hypotheses in a decreasing order of W_i
3. Initialize by setting:
 - $j := 1$ (j is the index of the set of hypotheses we currently consider)
 - $i_1 := 1, i_0 := 0$ (i_j is the number of hypotheses in \mathcal{H}_j)
 - $l := 0$ (l denotes the index of last drawn conjectured false null)
 - $\mathbf{f} := (0, 0, \dots, 0)$ (\mathbf{f}_i is the indicator of whether or not we conjecture H_i is a false null)
4. Estimate a_j , the number of false null hypotheses in $\mathcal{H}_j = \{H_i : i \leq i_j\}$, as

$$a_j := \left(\#\{i \leq i_j : L_i = 1\} - \#\{i \leq i_j : L_i = -1\} \cdot \frac{\lambda}{1-\lambda} \right) \vee 0.$$

Note that the first term is the number of original wins among the hypotheses in \mathcal{H}_j and the second is essentially the numerator of (3) (with $c = \lambda$), which uses the number of decoy wins to estimate the number of false discoveries among those original wins.

5. If $a_j > \|\mathbf{f}\|_1$ (the number of conjectured false nulls drawn so far) then draw $a_j - \|\mathbf{f}\|_1$ additional conjectured false nulls as follows:
 - (a) for each $i \in \{l+1, l+2, \dots, i_j\}$ let $w_i := 1 - \tilde{p}_i$, where \tilde{p}_i are the empirical p-values

- (b) while $a_j - \|\mathbf{f}\|_1 > 0$:
 - i. draw an index $i \in \{l+1, \dots, i_j\}$ according to the categorical distribution with a probability mass function proportional to w_i
 - ii. set $\mathbf{f}_i := 1$ and $w_i := 0$
- 6. If $i_j = m$ return the conjectured labels \mathbf{f} , else continue
- 7. Set $\delta_{j+1} := i_j - i_{j-1} + 1$ if no new conjectured false null were drawn in step 5, otherwise set $\delta_{j+1} := i_j - i_{j-1}$
- 8. Set $i_{j+1} := (i_j + \delta_{j+1}) \wedge m$
- 9. Set $j := j + 1$ and go back to step 4

Note that step 7 lets the data determine the number of hypotheses in $\mathcal{H}_{j+1} \setminus \mathcal{H}_j$: this number grows if going from \mathcal{H}_{j-1} to \mathcal{H}_j we concluded we do not need to draw any additional conjectured false nulls. This scheme is well adapted to handle a fairly common scenario where most of the highest scoring hypotheses are false null, making sure they will be labeled as such in our resamples.

The second phase of the algorithm simply resamples the indices in the usual bootstrap manner and then randomly permutes the conjectured true null scores:

1. independently sample m indices $j_1, \dots, j_m \in \{1, 2, \dots, m\}$
2. for $i = 1, \dots, m$:
 - (a) if $\mathbf{f}_{j_i} = 0$ draw a permutation $\pi_i \in \Pi_{d_1}$, else, $\mathbf{f}_{j_i} = 1$ so define $\pi_i := Id \in \Pi_{d_1}$ (the identity permutation)
 - (b) apply the permutation π_i to $\mathbf{V}_i := (\tilde{Z}_{j_i}^0 := Z_{j_i}, \tilde{Z}_{j_i}^1, \dots, \tilde{Z}_{j_i}^d)$: $\mathbf{V}_i \circ \pi_i := (\tilde{Z}_{j_i}^{\pi_i(1)-1}, \dots, \tilde{Z}_{j_i}^{\pi_i(d_1)-1})$
3. return the resampled labeled data $\{(\mathbf{V}_i \circ \pi_i, \mathbf{f}_{j_i}) : i = 1, \dots, m\}$

6.6 Labeled Bootstrap monitored Maximization (LBM)

Given the list of original and decoy scores, an ordered list of candidate methods \mathcal{M} , a fall-back method M_f , a set of considered FDR thresholds Φ , and the number of bootstrap samples n_b , LBM executes the following steps:

1. For each bootstrap/resample run $i = 1, \dots, n_b$:
 - (a) Generate a labeled resample as describe in Supplementary Section 6.5 above.
 - (b) Apply each method $M \in \mathcal{M}$ to the resample noting the number of discoveries $D_M^i(\alpha)$ for each $\alpha \in \Phi$, as well as the corresponding FDP, $F_M^i(\alpha)$ (computed based on the conjectured labels of the resample).
 - (c) For each $\alpha \in \Phi$ sort the methods according to $D_M^i(\alpha)$ with ties broken according to the rank of the methods in the list \mathcal{M} , and
 - i. record the rank $r_M^i(\alpha)$ of each method,
 - ii. record $F_*^i(\alpha) := F_M^i(\alpha)$ where M is the highest rank method (with the largest number of discoveries).

2. For each $\alpha \in \Phi$:

- (a) Estimate the FDR of the direct maximization approach as the simple average $\widehat{FDR}_*(\alpha) := \frac{1}{n_b} \sum_{i=1}^{n_b} F_*^i(\alpha)$.
- (b) If $\widehat{FDR}_*(\alpha) > \alpha$ (see the comment below) then
 - (the FDR of direct maximization seems too high so) set the selected method for this α to the fall-back method: $S(\alpha) := M_f$.

Otherwise,

- (direct maximization seems to work fine so) set the selected method to the one with the highest average rank: $S(\alpha) := \operatorname{argmax}_M \sum_{i=1}^{n_b} r_M^i(\alpha)$ (ties are broken according to the rank of the methods in the list \mathcal{M}).

We added to LBM two options that in practice were used throughout our reported simulations. The first is that we allowed some slack when comparing $\widehat{FDR}_*(\alpha)$ with α to check whether the FDR of direct maximization seems too high (step 2b above). Specifically, particularly because the empirical mean is taken over a relatively small number of resamples (we used $n_b = 50$ in our applications), we instead checked whether

$$\widehat{FDR}_*(\alpha) > \alpha + 4\sigma(\alpha) \cdot (1 - \hat{\pi}_0^*(\lambda)),$$

where $\hat{\pi}_0^*(\lambda)$ is the π_0 estimate used by FDS_1 described in Supplementary Sections 6.3 and 3.6, and $\sigma(\alpha)$ is the estimated standard error of $\widehat{FDR}_*(\alpha)$. In practice, this relaxation lead to some increase in power with no visible impact on the FDR control.

The second option is a post-processing step that aims to produce a monotone list of discoveries as a function of the FDR threshold α . Specifically, we check if the number of discoveries at α_{j+1} is smaller than the number we have when using $\alpha_j < \alpha_{j+1}$, and if that is the case, then we override our resampling-based selection of the optimal method for α_{j+1} and instead we use the same method that was previously selected for α_j , i.e., $S(\alpha_{j+1}) := S(\alpha_j)$.

In terms of the list of candidate methods we consider, \mathcal{M} , we need to strike a balance between considering more methods, equivalently more choices of (c, λ) , and the increasing likelihood that the fall-back would be triggered. In practice, we found that considering the methods of FDS_1 , mirror, and FDS (and in that the tie-breaking order, so FDS has the highest priority) works well so the reported version of LBM uses this particular list of methods.

6.7 Revisiting the failings of the canonical procedures

Going back to the two examples of Supplementary Section 6.1.1 we note that all our methods essentially control the FDR with the empirical FDR (FDP averaged over the 1K sets samples sets) below the selected FDR threshold for all $\alpha \in \Phi$ with a single exception in Example 1 at $\alpha = 0.2$, where FDS, FDS_1 , and LBM have an empirical FDR of 0.208: 4% over the threshold, compared with the $> 250\%$ violation of Storey with pooled p-values.

Interestingly, when comparing the power of our methods in Example 2, where BH applied to the pooled p-values made no true discoveries even at $\alpha = 0.65$, we find that both the mirror and FDS_1 are significantly weaker than FDS, LF and LBM, again demonstrating the utility of LBM. Specifically, at $\alpha = 0.15$ both FDS's and LBM's power stand at 78.5% and LF's at 62.8% compared

with 0% power for both the mirror and FDS_1 . At $\alpha = 0.2$ FDS, LBM, and LF boast 100% power while the mirror power stands at 0.1% and FDS_1 's power is 0.9%.

6.8 Analysis of real data

We applied our analysis to three datasets.

The human data set consists of a single control run (`CTL_R1_1` from the data set with MassIVE identifier `MSV000079437` (Zhong et al., 2016). The data was generated on an LTQ-Orbitrap Velos Pro on proteins extracted from human SH-SY5Y cells treated with 200 μ M H_2O_2 . The human reference proteome was downloaded from Uniprot on 28 Nov 2016.

The yeast data set was analyzed twice. The first, using a single run (`Yeast_In-gel_digest_2`) selected at random from the data set with PRIDE identifier `PXD002726` (Schittmayer et al., 2016). This is the yeast analysis that is reported in Figure 1. Because TDC reported 0 discoveries for 33 of the 100 decoys we drew, we performed a second analysis of the yeast data, this time using all three runs from the same PRIDE dataset. The data was generated on an LTQ Orbitrap Velos on proteins extracted from an in-gel digest of *S. cerevisiae* lysate. The yeast reference proteome was downloaded from Uniprot on 28 Nov 2016.

The ISB18 data set is derived from a series of experiments using an 18-protein standard protein mixture (<https://regis-web.systemsbiology.net/PublicDatasets>, (Klimek et al., 2008)). We use 10 runs carried out on an Orbitrap (`Mix_7`). The database consists of the 18 proteins from the standard mixture, augmented with the full *H. influenzae* proteome, as provided by Klimek et al.

Searches were carried out using the Tide search engine (Diament and Noble, 2011) as implemented in Crux (Park et al., 2008). The peptide database included fully tryptic peptides, with a static modification for cysteine carbamidomethylation (`C+57.0214`) and a variable modification allowing up to six oxidized methionines (`6M+15.9949`). Precursor window size was selected automatically with Param-Medic (May et al., 2017). The XCorr score function was employed for uncalibrated searches, using a fragment bin size selected by Param-Medic.

Clearly, the competition-based control of the FDR is subject to the variability of the drawn competing scores. To ameliorate this variability here, we initially searched the spectra against 100 randomly shuffled decoy databases, and then for each $d \in \{1, 3, 5, 7, 9\}$ we repeated our analysis drawing 100 sets, each with d of those decoy databases, while making sure that the 100 drawn sets are distinct. We can then compare the number of discoveries reported by each considered method at the selected FDR threshold α (here $\alpha \in \{0.01, 0.05, 0.1\}$). More precisely, for each number of decoys d we average the number of discoveries over the 100 randomly drawn sets of d decoys.

The ISB18 is a fairly unusual dataset in that it was generated using a controlled experiment, so the peptides that generated the spectra could have essentially only come from the 18 purified proteins used in the experiment. We used this dataset to get some feedback on how well our methods control the FDR, as explained next.

The spectra set was scanned against a target database that included, in addition to the 463 peptides of the 18 purified proteins, 29,379 peptides of 1,709 *H. influenzae* proteins (with ID's beginning with `gi|`). The latter foreign peptides were added in order to help us identify false positives: any foreign peptide reported is clearly a false discovery. Moreover, because the foreign peptides represent the overwhelming majority of the peptides in the target database (a ratio of 63.5 : 1), a native ISB18 peptide reported is most likely a true discovery (a randomly discovered peptide is much more likely to belong to the foreign majority). Taken together, this setup allows us to gauge the

actual FDP for each set of d drawn decoys, FDR threshold α , and the FDR controlling procedure that generated the discovery list. More precisely, we average the FDP over the 100 drawn sets of d decoys.

The 87,549 spectra of the ISB18 dataset were assembled from 10 different aliquots, so in practice we essentially have 10 independent replicates of the experiment. However, the last aliquot had only 325 spectra that registered any match against the combined target database, compared with an average of over 3,800 spectra for the other 9 aliquots, so we left it out when we independently applied our analysis to each of the replicates. By averaging the above decoy-drawn averaged FDP over the 9 aliquots we obtain an estimate of the FDR that we can compare to the selected FDR threshold.

Similarly, when gauging the power of a method on the ISB18 dataset our analysis was separately applied to each aliquot and then averaged over the aliquots.

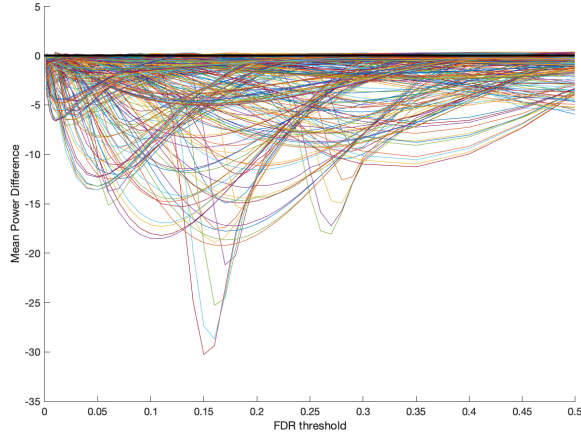
6.9 Conditional null exchangeability

The following condition which is a generalization of the conditional exchangeability property of Barber and Candès (2015) is weaker than the iid decoys condition. Nevertheless, it can be shown that it is sufficient for our statements to hold.

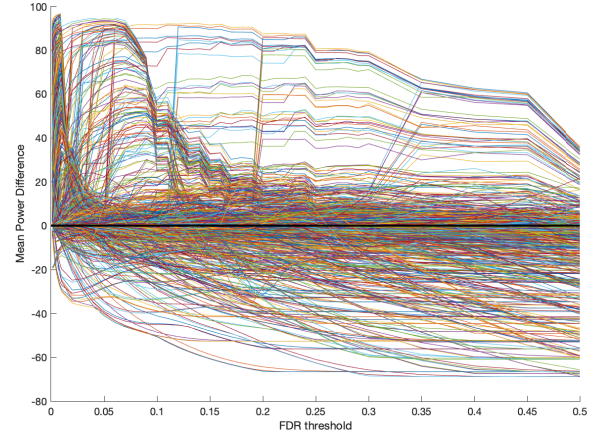
Definition 3. Let $\mathbf{V}_i := (\tilde{Z}_i^0, \tilde{Z}_i^1, \dots, \tilde{Z}_i^d)$, where $\tilde{Z}_i^0 := Z_i$ is the i th original score and $\tilde{Z}_i^1, \dots, \tilde{Z}_i^d$ are the corresponding d decoy scores, and let Π_{d_1} denote the set of all permutations on $\{1, \dots, d, d+1 =: d_1\}$. With $\pi \in \Pi_{d_1}$ we define $\mathbf{V}_i \circ \pi := (\tilde{Z}_i^{\pi(1)-1}, \dots, \tilde{Z}_i^{\pi(d_1)-1})$, i.e., the permutation π is applied to the indices of the vector \mathbf{V}_i rearranging the order of its entries. Let $N \subset \{1, 2, \dots, m\}$ be the indices of the true null hypotheses and call a sequence of permutations π_1, \dots, π_m with $\pi_i \in \Pi_{d_1}$ a *null-only sequence* if $\pi_i = Id$ (the identity permutation) for all $i \notin N$. We say the data satisfies the *conditional null exchangeability property* if for any null-only sequence of permutations π_1, \dots, π_m , the joint distribution of $\mathbf{V}_1 \circ \pi_1, \dots, \mathbf{V}_m \circ \pi_m$ is invariant of π_1, \dots, π_m .

6.10 Figures

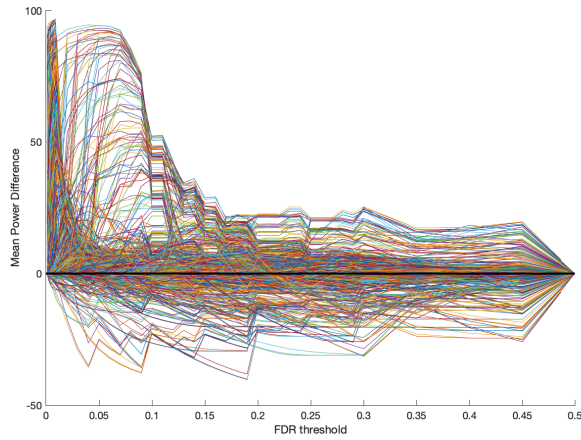
A: randomized (φ_u) vs. mirror (φ_m); $\lambda = c = 1/2$



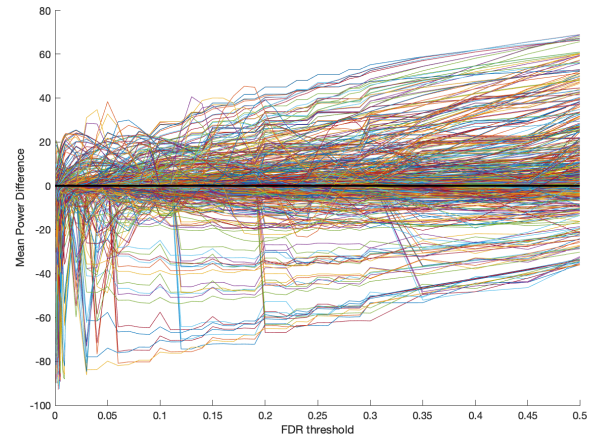
B: max vs. mirror



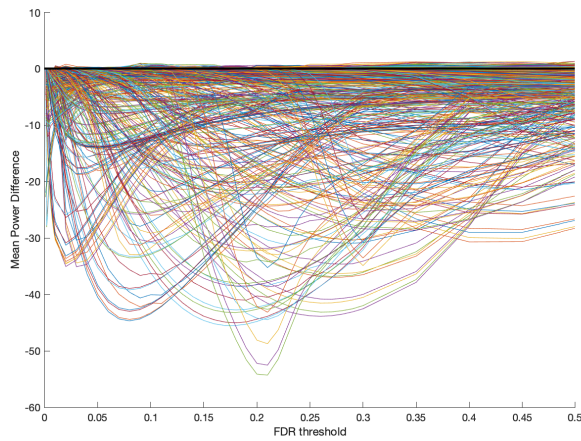
C: LF vs. mirror



D: LF vs. max



E: TDC vs. mirror



F: TDC vs. max

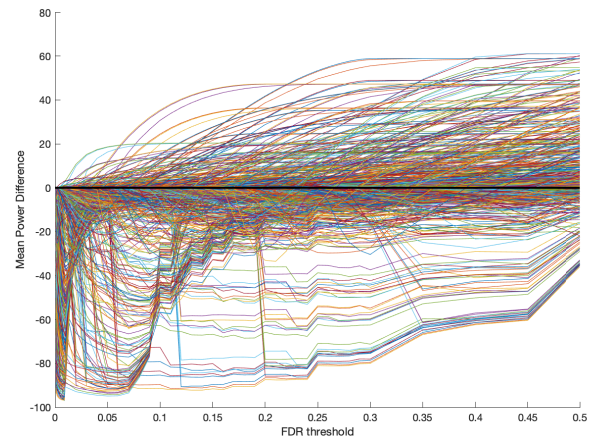


Figure 2: **Power difference.** Each of the panels show the difference in the average power of the two compared methods (positive values indicate the first method is more powerful). Each panel is made of 1200 curves, each of which shows the difference in power averaged over the 10K (100K for panel A) sets. The sets were drawn simulating both calibrated and non-calibrated scores using the experiment-specific parameter combination as described in Supplementary Section 6.2. The power of each method is the 10K-average (100K for panel A) percentage of false nulls that are discovered at the given FDR threshold. Note that figures' y-axes are on different scales. **(A:)** with $c = \lambda = 1/2$ the mirror map (φ_m) is consistently better than the randomized uniform map (φ_u); 100K draws for each of the 1200 parameter combinations. **(B-D:)** for each of the mirror, max, and LF procedures there are numerous cases where its power is significantly below one of the other methods. **(F:)** the mirror is consistently better than TDC. **(E:)** the max is not consistently better than TDC.

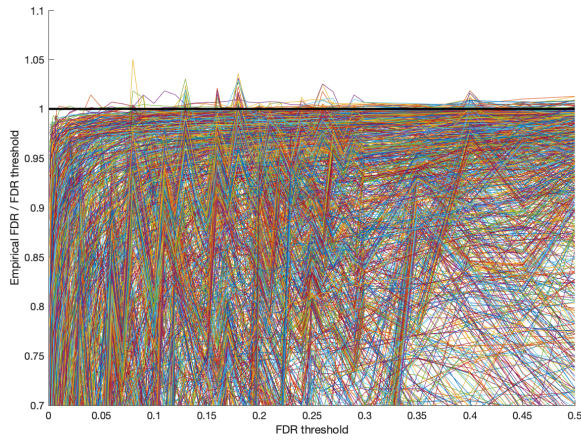
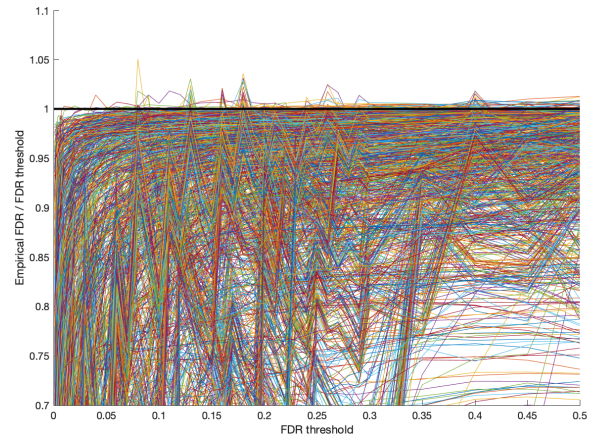
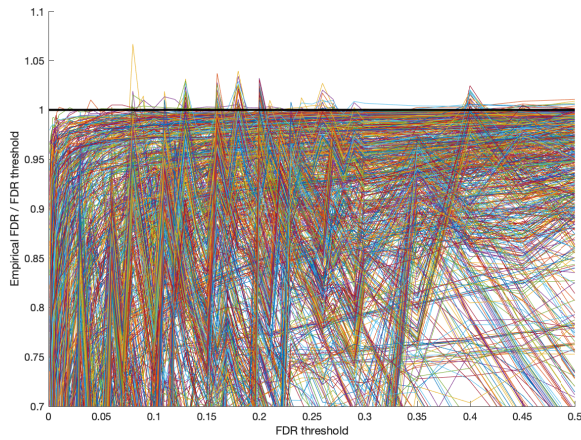
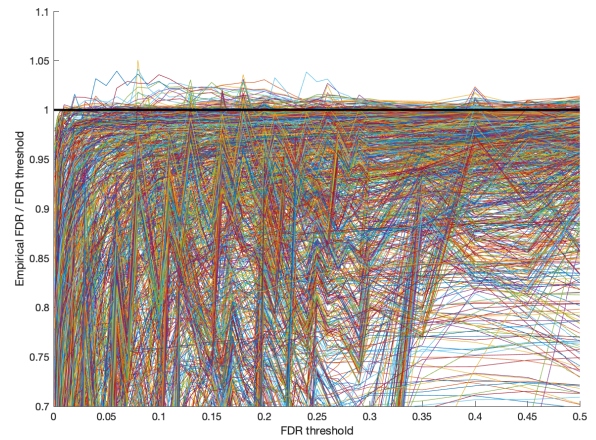
A: FDS**B: FDS₁****C: max****D: LBM**

Figure 3: FDR control. The panels show the ratio of the empirical FDR to the selected FDR threshold, and each is made of 1200 curves, each of which corresponds to one experiment involving 10K randomly drawn sets. The empirical FDR is the 10K-sample average of the FDP of each method's discovery list at the selected FDR threshold. The 10K sets were drawn simulating both calibrated and non-calibrated scores using the experiment-specific parameter combination as described in Supplementary Section 6.2. Notably there are relatively few cases where the empirical FDR is above the threshold (ratio > 1), and it is instructive to compare the ones observed in FDS, FDS₁ and LBM with those we note in the max method. Specifically, the overall maximal observed violation is 5.0% for FDS, FDS₁ and LBM while it is 6.7% for max. Similarly, the number of curves (out of 1200) in which the maximal violation exceeds 2% is 7 for FDS and FDS₁, 21 for LBM, and 24 for the max. Given that the max provably controls the FDR these simulations suggest that FDS, FDS₁ and LBM essentially control the FDR as well.

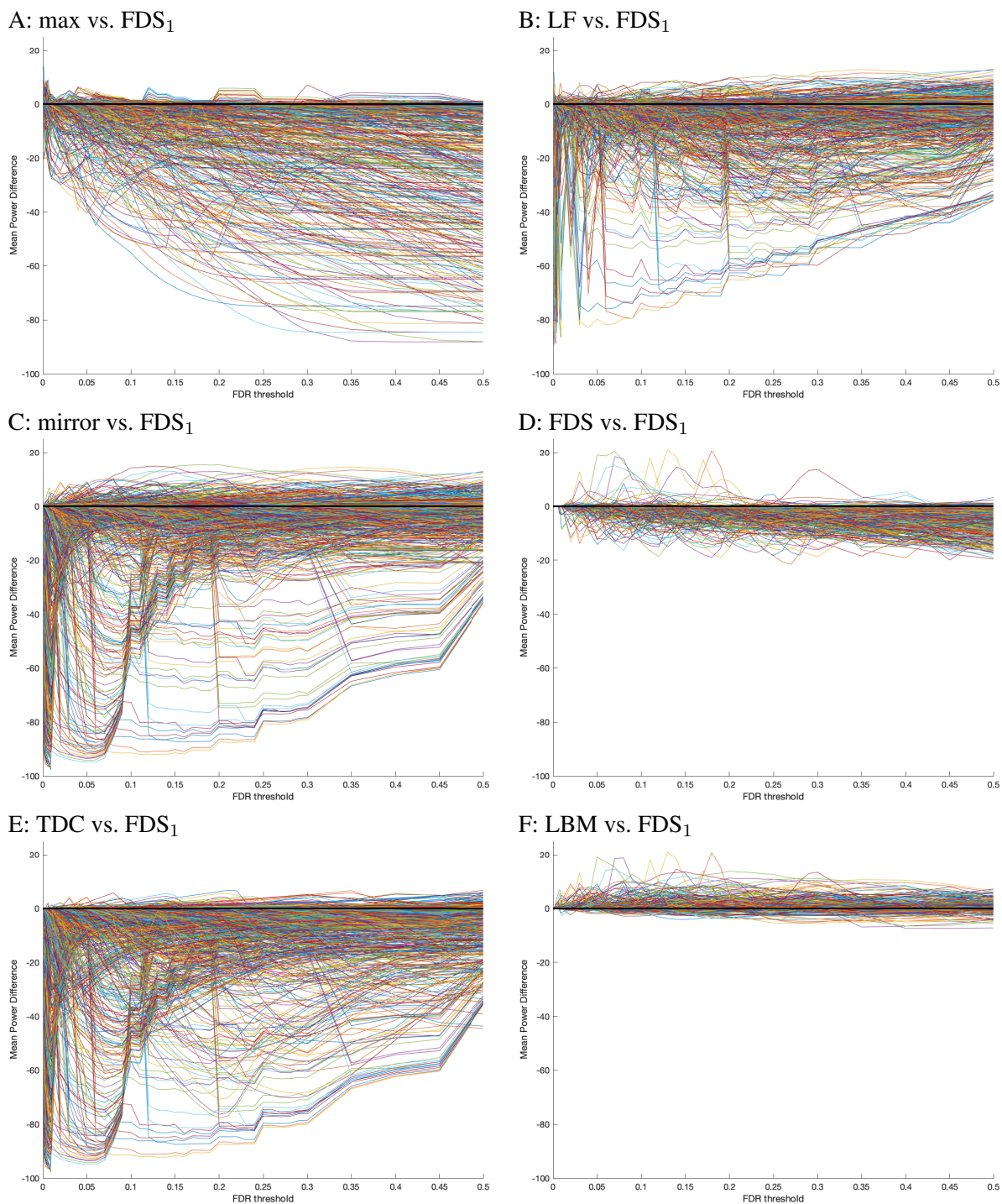
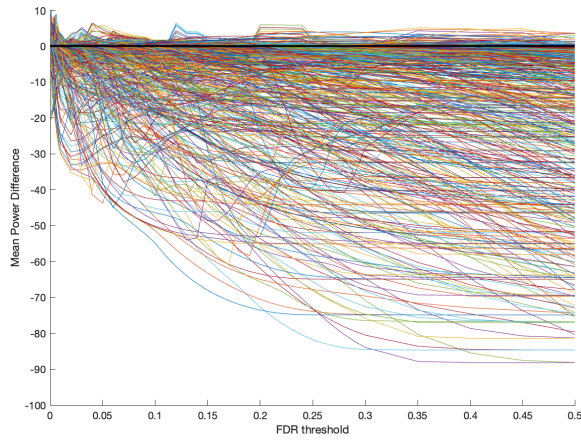
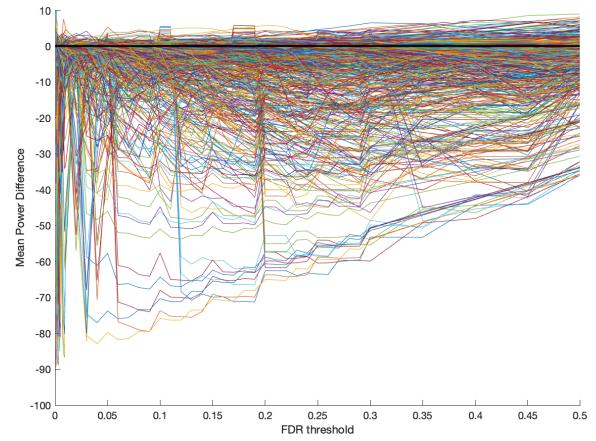


Figure 4: **Power relative to FDS₁**. Each of the panels show the difference between the average power of the noted method and FDS₁ (negative values indicate FDS₁ is more powerful). Each panel is made of 1200 curves, each of which shows the difference in power averaged over the 10K sets. The sets were drawn simulating both calibrated and non-calibrated scores using the experiment-specific parameter combination as described in Supplementary Section 6.2. The power of each method is the 10K-average percentage of false nulls that are discovered at the given FDR threshold. **(A-E):** FDS₁ arguably offers the best compromise among the multi-decoy procedures of mirror, max, LF, and FDS, as well as the single decoy TDC. **(F):** LBM seems to offer an overall more powerful procedure.

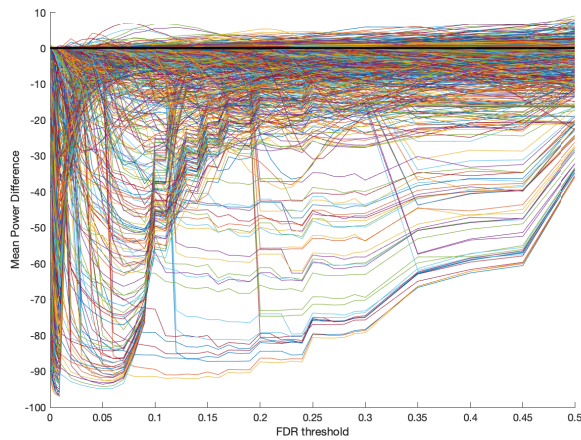
A: max vs. LBM



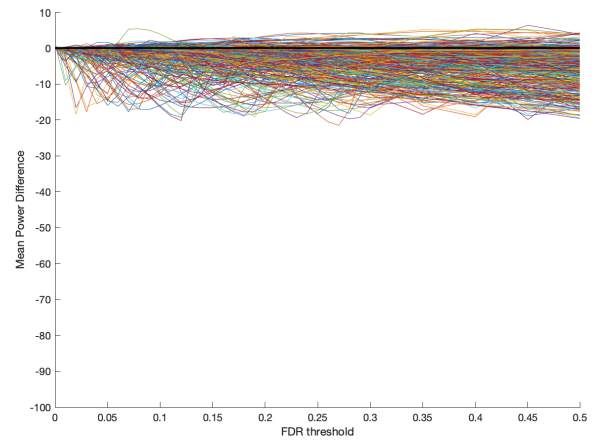
B: LF vs. LBM



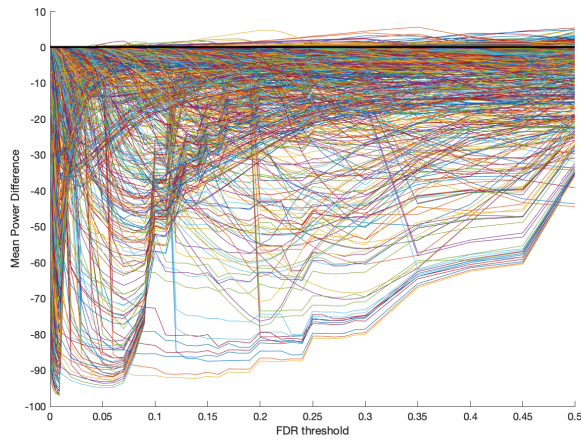
C: mirror vs. LBM



D: FDS vs. LBM



E: TDC vs. LBM



F: aTDC vs. LBM

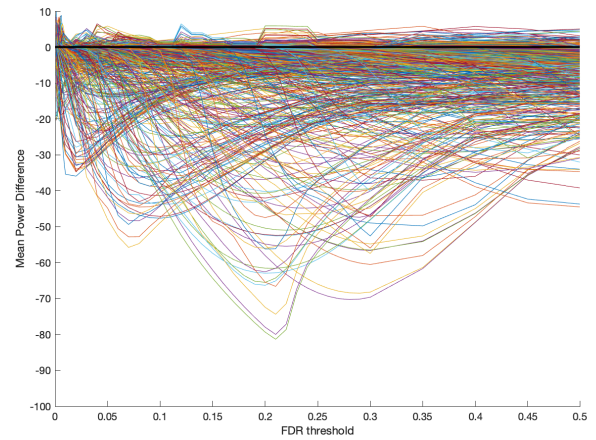


Figure 5: **Power relative to LBM.** Each of the panels shows the difference between the average power of the noted method and LBM (negative values indicate LBM is more powerful). For LBM vs. FDS_1 see panel F of Supplementary Figure 4. Each panel is made of 1200 curves, each of which shows the difference in power averaged over the 10K sets. The sets were drawn simulating both calibrated and non-calibrated scores using the experiment-specific parameter combination as described in Supplementary Section 6.2. The power of each method is the 10K-average percentage of false nulls that are discovered at the given FDR threshold. LBM seems to offer an overall optimal procedure among the competition-based procedures considered here.